THESIS FOR THE DEGREE OF DOCTOR OF PHILOSOPHY

Method Development for Signatures in Nuclear Material for Nuclear Forensic Purposes

ANNA VESTERLUND

Department of Chemistry and Chemical Engineering

CHALMERS UNIVERSITY OF TECHNOLOGY

Gothenburg, Sweden, 2019

Method Development for Signatures in Nuclear Material for Nuclear Forensic Purposes
ANNA VESTERLUND
ISBN 978-91-7905-197-6

Doktorsavhandlingar vid Chalmers tekniska högskola
Ny serie nr 4664
ISSN 0346-718X

Department of Chemistry and Chemical Engineering
Chalmers University of Technology
SE-412 96 Gothenburg
Sweden
Telephone + 46 (0)31-772 1000

Cover: A piece of uranium metal used in the nuclear forensic exercise CMX-6.
Photo by Ellinor Algin, Swedish National Forensic Centre (NFC)

Chalmers Reproservice
Gothenburg, Sweden, 2019

METHOD DEVELOPMENT FOR SIGNATURES IN NUCLEAR MATERIAL FOR NUCLEAR FORENSIC PURPOSES

ANNA VESTERLUND

Nuclear Chemistry
Department of Chemistry and Chemical Engineering
CHALMERS UNIVERSITY OF TECHNOLOGY

CBRN Defence and Security
SWEDISH DEFENCE RESEARCH AGENCY

Abstract

Nuclear forensics is a scientific discipline where signatures in nuclear and other radioactive material are investigated and evaluated in order to aid in criminal investigations concerning these materials. Examples of signatures that may be useful is the age and isotopic composition of the nuclear material and trace elements in the material. In order for evidence to hold up in court, the information extracted from forensic investigations need to be accurate and precise.

This work shows some possibilities and limitations of using two common techniques for measurements of nuclear material and other radioactive material: gamma spectrometry and inductively coupled plasma - mass spectrometry. One part of this work is dedicated to the applicability of hand-held instruments. The categorization of uranium using low-resolution gamma spectrometry and possibility of using signatures in high activity ^{241}Am sealed sources that can be obtained by HPGe were explored. In the other part, methods for high confidence measurements of lanthanides using ICP-MS were developed and problems arising when performing these analyses with as small uncertainties as possible were investigated.

The results show that nuclear forensic analyses require deep understanding in the measurement process in order to provide accurate results. Low-resolution instruments in the current configuration have been shown to be a poor choice for categorization of uranium. On the other hand, there are a number of interesting signatures in ^{241}Am-sources that can be provided by high-resolution gamma spectrometry. By using chemical separations or desolvating sample introduction systems in combination with careful data evaluation, it is possible to measure the lanthanide series without spectral interferences and with low uncertainties. By investing meticulous work to the analyses, it is possible to achieve measurements with high confidence.

Keywords: Nuclear forensics, Uranium, Lanthanide patterns, ^{241}Am, ICP-MS, gamma spectrometry

If a model is simple, it likely will be wrong, if it is complex, it surely is impractical.

- Unknown

LIST OF PUBLICATIONS

This thesis is based on the work contained in the following papers:

Paper I

Vesterlund, A., Ulvsand, T., Lidström, K., Skarnemark, G., Ekberg, C., Ramebäck, H.,
On the categorization of uranium materials using low-resolution gamma ray spectrometry,
Appl. Radiat. Isot., 72 (2013) 54–57.

Contribution: Main author, evaluation of experimental data.

Paper II

Vesterlund, A., Chernikova, D., Cartemo, P., Axell, K., Nordlund, A., Skarnemark, G., Ekberg, C., Ramebäck, H., Characterization of strong ^{241}Am sources, Appl. Radiat. Isot., 99 (2015) 162–167.

Contribution: Main author, evaluation of experimental data.

Paper III

Vesterlund A., Ramebäck H., Avoiding polyatomic interferences in measurements of lanthanides in uranium material for nuclear forensic purposes, J Radioanal. Nucl. Chem., 321 (2019) 723-731.

Contribution: Main author, all experimental work, all evaluation of experimental data.

Paper IV

Vesterlund A., Ramebäck H., Achieving confidence in trace element analysis for nuclear forensic purposes: ICP-MS measurements using external calibration. Accepted for publication in Journal of Radiochemical and Nuclear Chemistry.

Contribution: Main author, all experimental work, all evaluation of experimental data.

TABLE OF CONTENTS

1 INTRODUCTION

Nuclear material has been under strong worldwide regulation for over 60 years. Ever since the first military use of fission was realised as a result of the Manhattan project, the implications of such a weapon have been feared. The safeguards organization under the International Atomic Energy Agency (IAEA) has the main responsibility to ensure that member states maintain accountability of nuclear material kept within their borders. Even so, there have been incidents where nuclear material has been found out of regulatory control [Wallenius et al., 2006; Wallenius et al., 2007; Keegan et al., 2014]. Between 1993 and early 2019, the IAEA Incident and Trafficking Data Base (ITDB) has reported 3387 incidents involving nuclear material or other radioactive material out of regulatory control. Of these incidents, 759 have been associated with criminal activity and 16 of the criminal events have involved nuclear material usable for nuclear weapons (highly enriched uranium or plutonium) [ITDB, 2019].

Whereas the safeguards organization is meant to prevent incidents involving nuclear material, there is also a need for bringing actors who have handled nuclear material illegally to justice [UNSCR 1540, 2004]. The purpose of legal proceedings may be twofold: deterrence and retribution. The deterrence is directed against both non-state actors as well as against states. Since production of nuclear material is both resource demanding and a complex process, state involvement and a state's knowledge of the presence of nuclear material production is considered unavoidable. A confiscation of nuclear material found out of regulatory control would imply that a state has failed to follow international resolutions and agreements such as UNSCR 1540 [2004] concerning nuclear material. This concern would reinforce a state's will to control nuclear material and thereby deter from both negligence and proliferation. To help in these legal proceedings there has been a need for forensic science that focuses on the information that can be provided from the nuclear material itself, to complement traditional forensic evidence.

Nuclear forensic science is a scientific discipline that has been developing for the last 25 years, following the surge of cases of illicit trafficking of nuclear material after the dissolution of the Soviet Union. The aim of nuclear forensics is to aid criminal investigations concerning nuclear- or other radioactive material to find the origin and intended use of the seized material, i.e. the attribution. Commonly, the investigated material is nuclear material such as uranium and plutonium, but also radioactive sources may be the subject of investigation. Furthermore, there are other radionuclides, such as ^{241}Am, that are fissionable and hence sometimes referred to as alternative nuclear material [IAEA, 2002].

1.1 OBJECTIVES

The objective of the work presented in this thesis has been to investigate and develop signatures that may be useful in the field of nuclear forensics using gamma spectrometry and mass spectrometry as measurement techniques. For nuclear material, both techniques can be used. Gamma spectrometry is a robust, fairly quick, non-destructive technique but requires macroscopic amounts of material to be useful. Mass spectrometry, on the other hand, provides accurate and precise results with very small amounts of material, but is a destructive technique that often requires extensive sample preparation such as dissolution of the material followed by chemical separations. For solid-sample mass spectrometric techniques, such as laser ablation and SIMS, the sample preparation is minimal. However, a practical requirement for measuring radionuclides using mass spectrometry is that the

nuclides have sufficiently long half-lives. Another advantage of mass spectrometry is, of course, that non-radioactive elements, such as certain trace elements, also can be measured.

The first two papers concern measurements of radioactive material using hand-held gamma spectrometry. These gamma detectors are commonly used by first-responders or customs, or in early stages of a nuclear forensic investigation, i.e. in the detection and identification as well as in a basic characterization of the material at e.g. the site of incident. **Paper I** shows some of the difficulties when attempting to categorize uranium using low-resolution gamma spectrometry and intends to explain why categorizations may be erroneous. Furthermore, the risk of making erroneous decisions based on low-resolution measurements is highlighted. **Paper II** shows what kind of characteristics can be extracted from a simple high-resolution gamma spectrometric measurement of a strong radioactive source containing the alpha-emitter ^{241}Am. These characteristics could be included in a National Nuclear Forensics Library (NNFL) to help identify a radioactive source found out of regulatory control.

The last two papers deal with measurements of stable elements in uranium material using ICP-MS that can be used for either origin attribution or for comparison between different materials. In **Paper III,** a comparison is made between interfered and interference-free measurements. The paper shows two methods to produce precise and interference-free lanthanide patterns using ICP-MS for uranium attribution. **Paper IV** shows that by decreasing the measurement uncertainty in trace element measurements to be able to compare small differences in analyte concentration of stable elements for nuclear forensic purposes, it can be shown that certified reference materials may have underestimated uncertainties and/or a concentration bias. The paper also shows the difference between using ordinary least squares regression, which is frequently applied to external calibration in the literature, and weighted least squares regression, which is the correct statistical approach for evaluation.

2 BACKGROUND

2.1 THE POLITICAL HISTORY OF NUCLEAR EVENTS

In 1938 Otto Hahn and Fritz Strassmann irradiated uranium with neutrons and discovered that one resulting entity from the irradiations was barium, but they could not explain how this was possible [Hahn and Strassmann, 1939]. Shortly after, Lise Meitner and her nephew Otto Frisch devised the theoretical explanation that the neutron irradiation splits the uranium atom into two nuclei of roughly equal size, which would explain the presence of barium observed by Hahn and Strassmann. They also explained that energy is released in the process [Meitner and Frisch, 1939]. By this, fission was discovered and shortly after, it was found that the neutrons produced in the fission could cause a chain reaction [Zinn and Szilard, 1939]. In the Frisch-Peierls memorandum, written in 1940, Rudolf Peierls and Otto Frisch presented the first technical description of the possibility of utilizing the fission chain reaction in a bomb construction using uranium enriched in ^{235}U [Arnold, 2003], and July 16 1945, the first nuclear test, the "Trinity" test, was conducted in New Mexico, U.S. The test was followed by the atomic bombs over Hiroshima and Nagasaki shortly after. Soon, technical details on the construction of the atomic bomb leaked to the Soviet Union, and when the Soviet Union had implemented the nuclear weapons technology in 1949, when the first Soviet test was conducted, the nuclear arms race became a part of the Cold War.

The IAEA was established in 1957 after the "Atoms for Peace" initiative by the U.S. president Dwight D. Eisenhower to promote peaceful use of nuclear energy and to prevent nuclear material to be used for military purposes [Fischer, 1997]. The original idea was that the IAEA would serve as a bank for nuclear material. A safeguards organization was created to ensure that nuclear material was not used for military purposes. However, the Cold War prevented the implementation of the IAEA as a nuclear material protector. Instead, while the nuclear technology intended for peaceful purposes spread across the world, so did the nuclear weapons technology. For example, the plutonium used for the Indian nuclear weapons programme was produced in a research reactor supplied by Canada [Fischer, 1997]. By 1968, five countries around the world had nuclear weapons technology and, furthermore, conducted nuclear weapons tests. It became clear that the spread of this knowledge and technology had to be stopped. In 1970, the Nuclear Non-Proliferation Treaty (NPT) entered into force.

2.2 NUCLEAR SECURITY

The NPT can be described as having three pillars: non-proliferation, disarmament, and peaceful use of nuclear technology. The first part, non-proliferation, obligates the nuclear weapons states not to share nuclear weapons or technology related to nuclear weapons with states that do not have nuclear weapons. Furthermore, non-nuclear weapons states are obligated not to receive or develop nuclear weapons technology. In addition, non-nuclear weapons states are obligated to accept IAEA safeguards to verify that the nuclear technology within the state is used for peaceful purposes. The safeguards organization maintains credible assurance that nuclear material under safeguards is used for peaceful aims and is not converted into nuclear weapons [NPT/CONF.2015/13, 2015]. The second pillar, disarmament, implies that the nuclear weapons states are obligated to pursue the complete disarmament of nuclear weapons, and the third pillar gives the states the right to develop and use nuclear technology for peaceful purposes, e.g. nuclear energy [Reed and Stillman, 2009]. Despite the NPT, a few states have developed and tested nuclear weapons after the implementation of the treaty. After the disintegration of the Soviet Union, there were suddenly three new nuclear weapons states,

Belarus, Kazakhstan and Ukraine. However, these three states soon transferred their stock of nuclear weapons to the Russian Federation [Reed and Stillman, 2009]. In the aftermath of the breakup of the Soviet Union, seizures of illicit radiological and nuclear material at borders started to increase rapidly. Concerns that a black market for nuclear material was developing, resulted in the growing interest to be able to identify the origin of seized material, i.e. a forensic science focussed on nuclear and other radioactive materials [Mayer and Glaser, 2015].

After the 9/11 attacks, concerns were raised about the possibility for terrorists to use nuclear or other radioactive material for their objectives. Three ways for terrorist groups to obtain nuclear material have been proposed [Litwak, 2016]. One option, indigenous production, is that the terrorist group, without the aid of a state, could build a nuclear weapon. This option is considered unlikely due to the complexity and the technical skill needed to construct a nuclear weapon. Somewhat more likely is the event that a terrorist group obtains weapons grade nuclear material and weaponizes the material without the involvement of a state. The second option, transfer, is that a terrorist group acquires a functioning nuclear weapon, by the aid of a state. A third way for terrorists to acquire nuclear weapons is by "unintended leakage" such as theft and insider operations. A perhaps more likely event is the antagonistic use of radioactive sources in combination with explosives, so called Radiological Dispersion Devices (RDD), or more colloquially "dirty bombs", where the explosives are used to disperse radioactive material in a selected location. These events may not be as disastrous as a nuclear weapon detonation but on a psychological level, it has been suggested that the fear spread by such a device may be as serious as that caused by a nuclear device [Litwak, 2016].

While terrorist groups may not be deterred from using nuclear weapons by threat of retaliation from the international community, the proliferation of nuclear weapons may be prevented by deterring states from, by either neglect or intention, conveying nuclear weapons or nuclear weapons material to terrorist organisations. Under the threat of the possibility to attribute nuclear material, found out of regulatory control, to a certain state, states will be forced to comply with international agreements by maintaining nuclear security to avoid retaliation from either the international community or another state [Litwak, 2016].

A number of initiatives have been realised to highlight the importance of nuclear security. The Global Initiative to Combat Nuclear Terrorism (GICNT) was initiated in 2006 as a joint effort between Russia and the United States. The aim of GICNT is to strengthen the global capability to prevent, detect and respond to nuclear terrorism. The organization is open to any state that is committed to implementing the eight principles in the Statement of principles [GICNT, 2018]. As of early 2019, 88 nations and 6 organizations were members.

To handle events with nuclear material and other radioactive material out of regulatory control, the IAEA has established a nuclear security programme. This programme focuses on prevention and detection of and response to criminal or other unauthorized acts involving nuclear or other radioactive material [IAEA, 2011]. The IAEA recommends each state to implement a nuclear security infrastructure to protect nuclear and radioactive material within its borders. The state should also have the ability to "prevent, detect and respond to nuclear security events" [IAEA, 2015]. The preventive measures involve deterrence, ensuring information security and trustworthiness of personnel by the implementation of a "nuclear security culture". The detection measures should involve detection by instruments as well as information alerts. The response measures involve the actions that follow a detected nuclear security event and includes notification and activation of all relevant authorities including the initiation of investigations concerning the event. For the purpose of both deterrence and response, nuclear forensics plays an important part.

2.3 NUCLEAR FORENSICS

The aim of nuclear forensics is to find the attribution of unknown nuclear and other radioactive material. The attribution assessment is used to determine the origin of the material, the intended use and the responsible individuals connected to the material [Hutcheon et al., 2013]. Methodology in nuclear forensics includes measurements of radioactive nuclides as well as stable elements that can be used to link a material to another material, facility or even a geographical location. Many methods in nuclear forensics are based on methods used in other disciplines such as age dating and lanthanide analysis, both commonly employed in geology [Cheong et al., 2015; Lobato et al., 2015]. However, a major difference between nuclear forensics and, for instance, geology is the need for quality assurance to meet the high legal and scientific scrutiny [Leggitt et al., 2009]. Therefore, a considerable amount of the conducted research focuses on improving the measurement accuracy and minimizing uncertainties [Williams et al., 2014]. Nuclear forensics often combines laboratory methods used for ordinary analysis of nuclear and other radioactive material and interpretation of the analysis results to provide technical conclusions about, for example, seized illicit nuclear or radioactive materials [Kristo and Tumey, 2013].

A nuclear forensic investigation can be divided into three parts [IAEA, 2006]:

- Categorization

The IAEA report "Nuclear Forensics Support" [2006] states that "*categorization is used to address the threat posed by a specific incident*". The aim of the categorization is to identify the safety risk to first responders and to the public, as well as to evaluate whether the incident is part of criminal activity and/or a threat to national security. One example of need for categorization may be the interception of uranium at a border control. The categorization done at this stage could include gamma spectrometric measurements of the material. Measuring the enrichment of the uranium would provide information on how to proceed with confiscation or even if a crime has been committed.

- Characterization

Characterization handles the determination of specific characteristics of the material. Table 1 lists some useful techniques and methods and gives a recommended sequencing of analysis to give the most valuable information early in an investigation without limiting the possibility of subsequent analyses [IAEA, 2015]. The table is a recommendation from the Nuclear Forensics International Technical Working Group (ITWG), which is an association of nuclear forensics practitioners. Important nuclear forensic characteristics include isotopic and elemental composition and physical characteristics.

The isotopic composition analysis can be performed using gamma or alpha spectrometry or any of the mass spectrometric techniques depending on sample size [Ramebäck et al., 2012]. The isotopic composition provides information about the intended use of the nuclear material but can also reveal if e.g. a uranium material is reprocessed [Zsigrai et al., 2015]. Elemental composition, or impurity measurements, is the measurement of remaining elemental impurities and can be used to explain the production process of the nuclear material or the geographical origin of the source material [Healy and Button, 2013; Varga et al., 2010a]. Physical characterization is used to tell the grain size or the chemical phase of a material and is mainly performed using surface characterization techniques such as scanning electron microscopy (SEM) and x-ray diffraction (XRD) but also other, more basic techniques, such as dimensions, mass determination and density measurements [Holmgren Rondahl et al., 2018; Sweet et al., 2013]. Another useful characteristic is the age of a material, i.e. the time that has passed since the last separation. The idea of age dating is to investigate the relation between a mother nuclide and the ingrowth of a daughter nuclide [Eppich et al., 2013; Gehrke and East, 2000; Nygren et al., 2007; Ramebäck et al., 2008; Varga et al., 2011]. The principles of age dating are explained in Chapter 3.

Table 1 Suggested priorities for common characterization methods [IAEA, 2015].

Techniques/Methods	24 h	One week	Two months
Radiological	Dose rate		
	Surface contamination		
	Radiography		
Physical	Visual inspection	SEM	TEM
	Photography	XRD	
	Mass determination		
	Dimensions		
	Optical microscopy		
	Density		
Traditional forensics	Collection of evidence		Analysis and interpretation
Isotope analysis	Gamma spectrometry	TIMS	SIMS
		ICP-MS	Radiometric techniques
Radiochronometry	Gamma spectrometry (for Pu)	TIMS	Gamma spectrometry (for U)
		ICP-MS	Alpha spectrometry
Elemental/chemical analysis	XRF	ICP-MS	GC-MS
		IDMS	
		FTIR	
		Assay (Titration, IDMS)	
		SEM/X ray spectrometry	

- Nuclear Forensic Interpretation

The results acquired in the characterization are used in the nuclear forensic interpretation where possible connections between materials and events are evaluated. Nuclear forensic analysis can be divided into two groups: comparative and predictive analysis [Hutcheon et al., 2013]. A measurement technique or a measurand can be used both for comparative and predictive analysis, depending on the question. The comparative analyses can be used to answer questions such as "Do these materials have the same origin?" or "Does this material correspond to any material in the database or any material we have knowledge about?" The predictive analyses, on the other hand, can be used to explain the origin of the material, processes the material has undergone and intended use of the material. For example, the isotopic composition can be used to compare different samples to see whether it is likely that they are originating from the same batch, but the composition can also be used to explain the intended use of the material and possibly the production process. Thus, the nuclear forensic interpretation is used for both linking materials and events to each other, and for the determination of the intention of the nuclear security event. The nuclear forensic interpretation requires highly skilled experts, so called subject matter experts (SME), who can interpret the analysis results and assess the significance of the findings [Mayer and Glaser, 2015].

2.3.1 National Nuclear Forensics Libraries

The IAEA encourages its member states to implement a national system for identification of nuclear and other radioactive material found out of regulatory control, to support nuclear security and non-proliferation [IAEA, 2018]. To determine whether a seized material originates from a state, a register of the nuclear material and other radioactive material held within a country can be helpful. This register is often referred to as a National Nuclear Forensics Library (NNFL) and may consist of reference information regarding nuclear material and radioactive sources. Ideally, this compilation of data would be available to the international community, but due to the sensitive nature of the information, the aim is to keep the libraries at a national level. The IAEA, however, encourages information sharing between countries when needed, either by direct contact between states or by using an international organization as the intermediary [IAEA, 2018; Mayer and Glaser, 2015].

The library may contain information that can be used to compare with data from analyses in nuclear forensic investigations, as well as with information from manufacturers. It is also possible to include archive samples of different sources in the library to facilitate ad hoc comparisons of characteristics of an investigated material and samples in the archive [Wacker and Curry, 2011]. Another crucial part in an NNFL is subject matter expertise to aid in the determination of what information to include and how it should be interpreted [Borgardt et al, 2017]. The aim of the NNFL is to ensure that nuclear material and radioactive sources are identifiable and traceable, or when this is not feasible, ensure that there are alternative processes for identifying and tracing sources [IAEA, 2004; IAEA, 2015]. The complexity of the NNFL may depend on a state's nuclear and radioactive material holdings. The signatures could be used to compare with the NNFL in order to determine whether a seized material is consistent with material that has been produced, used or stored within a state.

3 THEORY

3.1 NUCLEAR FORENSIC SIGNATURES

3.1.1 Isotopic ratios

In categorization of nuclear material, isotopic ratio measurements provide the enrichment of e.g. uranium, which will reveal the intended use of the material. In characterization, the isotopic ratio measurements will provide means for the comparison of different materials and, in addition, reveal whether the material has been reprocessed or not. Isotopic ratio measurements can be performed with either radiometric or mass-spectrometric techniques depending on the nuclides in question.

3.1.2 Radiochronometry

Radiochronometry is an important tool for nuclear forensics as, unlike many other signatures, it is a predictive signature that does not necessarily need a comparison to other materials to be useful [Mayer and Glaser, 2015].

The time that has passed since the last chemical separation is referred to as the age of a nuclear or other radioactive material. The age can be assessed by measuring the relation between the mother nuclide and its progeny. The rationale is that, at the time of separation, only the mother nuclide is present, e.g. uranium nuclides or ^{241}Am while all daughter products have been completely removed in the separation process. With time, the daughter nuclides will grow in and by measuring the ratio between the mother and daughter nuclide, the age of the material can be calculated. When performing radiochronometry, a few assumptions have to be made. The first assumption is that, at the time of separation (t=0), all of the daughter nuclides are removed. The second assumption is that the material is contained in a closed system, i.e. as the daughter nuclides grow in they remain in the material and is not removed by any process [Sturm et al., 2014]. Since these assumptions may be difficult to confirm, the measured age, also called the model age may not be the same as the actual age, i.e. the sample age. Another requirement for radiochronometry is that the mother and daughter nuclide are in radioactive disequilibrium. This means that not all mother/daughter-pairs are useful for radiochronology.

Radioactive decay can be described according to:

$$\mathrm{X}_1 \overset{\lambda_1}{\rightarrow} \mathrm{X}_2 \overset{\lambda_2}{\rightarrow} \mathrm{X}_3 \overset{\lambda_3}{\rightarrow}_{\ldots} \tag{1}$$

where λ_i is the decay constant for radionuclide X_i. The age of a material, t, can, in the case of two successive decays, be calculated according to

$$t = \frac{1}{\lambda_1 - \lambda_2} \cdot \ln\left(1 - \left(1 - \frac{\lambda_1}{\lambda_2}\right)\frac{A_2}{A_1}\right) \tag{2}$$

where A_i is the activity of radionuclide X_i. The corresponding expression of the age performed by atom counting (mass spectrometry) is analogous to Eq. 2.

In cases where the half-life of the daughter X_3 is substantially shorter than the half-life of X_2, the X_3 activity will rapidly grow into secular equilibrium and equal that of X_2. This means that X_3 will decay with the half-life of X_2. In this case, it is possible to use the A_3/A_1 activity ratio together with the decay constant of X_2 in Eq. 2 to calculate the age of the material. This may be convenient in cases where the

gamma photon yield of radionuclide X_2 is too small to be detected with gamma spectrometry within reasonable measurement time. One such example is given in **Paper II**. The age determination of ^{241}Am was performed by using the granddaughter ^{233}Pa to ^{241}Am instead of its daughter ^{237}Np, since the photon emission probability of ^{237}Np are too small to be visible in a high activity ^{241}Am spectrum. The half-lives of ^{241}Am, ^{237}Np and ^{233}Pa are 432.6 y, $2.144 \cdot 10^6$ y and 26.98 d, respectively [DDEP, 2018].

3.1.3 Trace elemental impurities

Trace elemental impurities are elements found in a material that have not been deliberately added to the material [Lützenkirchen et al., 2019]. One common example in the field of nuclear forensics is trace elements found in uranium material. These impurities can either originate from the geological deposit and remain in the uranium ore concentrate (UOC) after milling, or from the various processes the material undergo. Therefore, the trace elements can be used both to compare materials to each other and to estimate the type of processes the material has passed [Varga et al., 2017]. Elements that have been added intentionally in the material and that are relevant for the properties of the material are called additives and are, in general, substantially more abundant than trace elements.

3.1.3.1 Lanthanide patterns

Lanthanide patterns have been considered a good predictor of geographical origin of uranium material for some time [Mercadier et al, 2011]. The lanthanide series comprises 15 elements, whereof 14 are naturally occurring. The 15th, promethium, does not have any stable isotopes and is therefore omitted from the lanthanide patterns. The composition of the lanthanides depends on the geological processes that the material have undergone. Examples of different lanthanide patterns are shown in Figure 1. The lanthanide patterns originate from different types of uranium ore formations. Due to environmental conditions, such as temperature and salinity during the ore formation process, the lanthanides will fractionate [Mercadier et al, 2011]. The reason why the lanthanide series is a good indicator for geographical origin is that all the lanthanides are trivalent under normal conditions and have similar characteristics. Therefore, the relative abundance of the lanthanides in a material remain, on a relatively short time scale, even though the material undergo various processes. The exceptions are cerium and europium that, additionally to the trivalent state, may be tetravalent and divalent, respectively.

The measured concentrations of lanthanides in a sample is often normalised to chondrite to allow for an easier interpretation of geological processes. The normalised values are then plotted in increasing atomic number to receive the lanthanide pattern. Chondrite is a meteoritic material that is assumed to represent the average concentrations of elements in the solar system, and the assumption is that the composition of the lanthanides on earth as a whole is the same as that of the chondrite meteorites. Due to various processes during the history of Earth, the lanthanides have fractionated [White, 2013; Prohaska et al., 1999]. By normalizing the lanthanides measured in a sample to chondrite values, geologists can use the information given by the pattern to explain the history and source of a rock [White, 2013]. Another reason for presenting the lanthanides as chondrite normalised abundances rather than absolute concentrations is that all odd-numbered elements, with only a few exceptions, are less abundant than their even-numbered neighbours, resulting in a saw tooth-shaped lanthanide pattern. The normalisation produces a smooth pattern that is more easily interpretable [White, 2013].

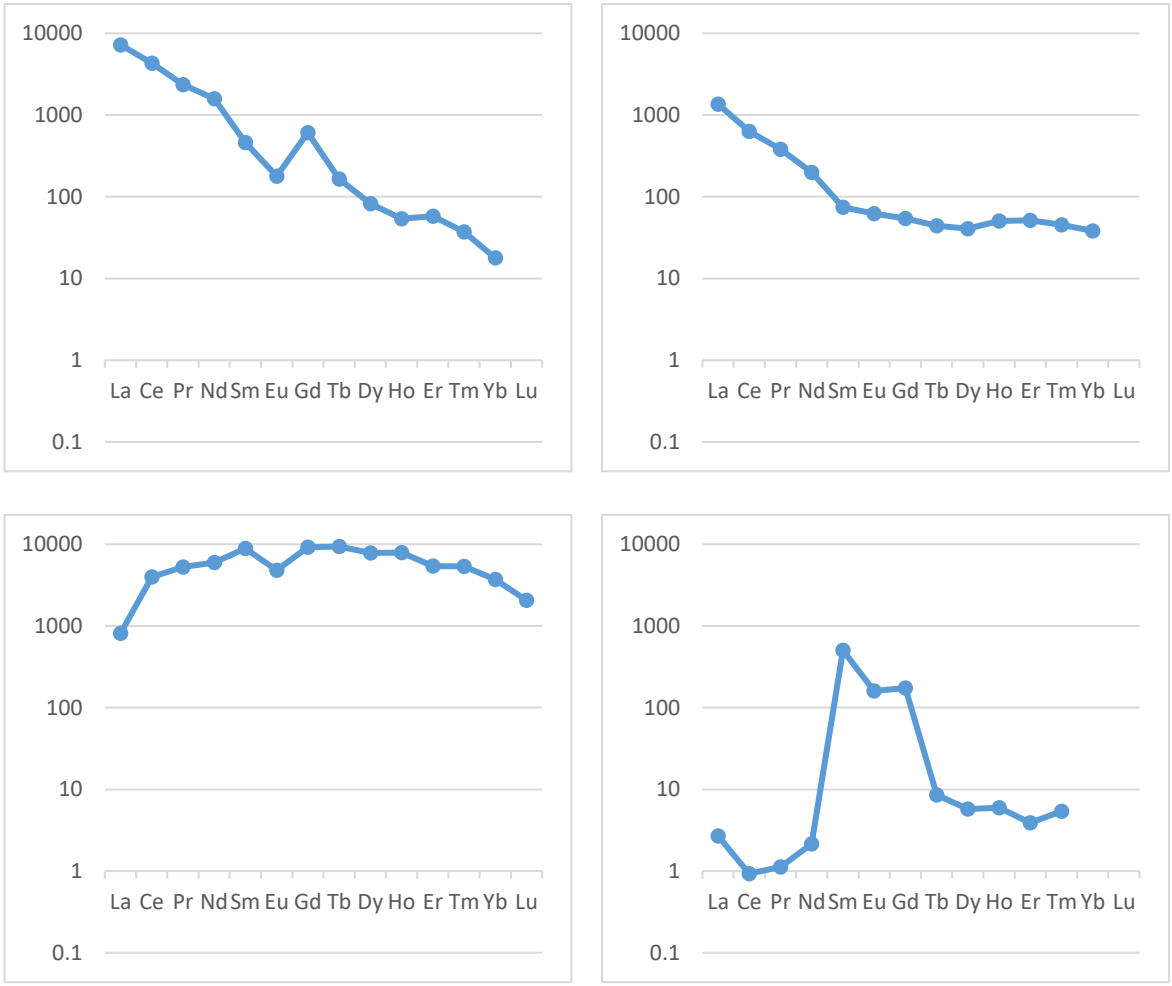

Figure 1 Examples of chondrite normalized lanthanide patterns from four different geographical origins. Top left: Vein-type from Commanderie, France, Top right: Roll-front from Kazakhstan, Bottom left: Synmetamorphic from Mistamisk and Bottom right: Volcanic-related from Streltsovskoye. Data from Mercadier [2011].

Uranium is commonly found as an oxide in nature. Due to their similar ionic radii, the elements in the lanthanide series are often found together with uranium in non-negligible amounts. Therefore, many papers have suggested lanthanide patterns as a good indicator of geographical origin of uranium [Frimmel et al., 2014; Fryer and Taylor, 1987; Mercadier et al., 2011; Spano et al., 2017; Varga et al., 2010a].

3.1.3.2 Measurements of lanthanides in uranium material

Due to the generally low abundance of lanthanides in uranium materials, lanthanide measurements require a measurement technique with low detection limits. Mass spectrometry is such a technique, even though there are some difficulties in measuring lanthanide concentrations using ICP-MS [Vaughan and Horlick, 1990; Dulski, 1994]. The heavy uranium matrix may cause matrix effects with a following decrease in measurement sensitivity and signal stability [Tan and Horlick, 1987; Beauchemin et al., 1987]. This will in turn increase the detection limits. The high amount of uranium introduced into the instrument may also cause memory effects, i.e. high uranium backgrounds that may be difficult to eliminate. To solve this problem Varga et al. proposed a method for group separation of the lanthanide series to remove uranium and barium from the samples using a resin based on CMPO/TBP (TRU resin) [2010b].

Many of the lanthanides have many isotopes and therefore there is a number of isobars among the lanthanides. There is, however, at least one isotope of each lanthanide free of isobars. Another problem with measuring lanthanides using ICP-MS is the presence of polyatomic interferences such as oxides and hydrides. Especially lighter lanthanides, such as cerium and praseodymium are prone to oxide formation. These oxides will interfere with the heavier lanthanides [Dulski, 1994; Longerich et al., 1987]. One such example is $^{141}Pr^{16}O^{+}$ that interferes with $^{157}Gd^{+}$. This may cause a problem since the lighter lanthanides often are more abundant than the heavier ones in uranium bearing material. The interference may then be a substantial part of the measured signal of the heavier elements. The lanthanides and their most prominent interferences can be seen in Figure 2. Each isotope is coloured in green, yellow or red to illustrate that quantification using the isotopes is suitable, suitable with caution and unsuitable, respectively. To be able to use the isotopes marked in yellow for accurate quantification, the interferences should be addressed [Vesterlund et al, 2014].

m/z	Ba	La	Ce	Pr	Nd	Sm	Eu	Gd	Tb	Dy	Ho	Er	Tm	Yb	Lu
130	0.11														
131															
132	0.1														
133															
134	2.42														
135	6.59														
136	7.85		0.19												
137	11.23														
138	71.7	0.089	0.25												
139	^{138}BaH	99.911													
140		^{139}LaH	88.45												
141			^{140}CeH	100											
142			11.11	^{141}PrH	27.2										
143			^{142}CeH		12.2										
144					23.8	3.1									
145					8.3										
146	^{130}BaO				17.2										
147	^{130}BaOH				^{146}NdH	15									
148	^{132}BaO				5.8	11.3									
149	^{132}BaOH				^{148}NdH	13.8									
150	^{134}BaO				5.6	7.4									
151	^{135}BaO				^{150}NdH	^{150}SmH	48								
152	^{136}BaO		^{136}CeO			26.7	^{151}EuH	0.2							
153	^{137}BaO					^{152}SmH	52								
154	^{138}BaO		^{138}CeO			22.7	^{153}EuH	2.18							
155	^{138}BaOH	^{139}LaO				^{154}SmH		14.8							
156		^{139}LaOH	^{140}CeO					20.47		0.056					
157			^{140}CeOH	^{141}PrO				15.65							
158			^{142}CeO	^{141}PrOH	^{142}NdO			24.84		0.095					
159			^{142}CeOH		^{143}NdO			^{158}GdH	100						
160					^{144}NdO	^{144}SmO		21.86	^{159}TbH	2.329					
161					^{145}NdO	^{144}SmOH		^{160}GdH		18.889					
162					^{146}NdO					25.475		0.14			
163					^{146}NdOH	^{147}SmO				24.896					
164					^{148}NdO	^{148}SmO				28.26		1.6			
165					^{148}NdOH	^{149}SmO				^{164}DyH	100				
166					^{150}NdO	^{150}SmO					^{165}HoH	33.5			
167					^{150}NdOH	^{150}SmOH	^{151}EuO					22.87			
168						^{152}SmO	^{151}EuOH	^{152}GdO				26.98		0.12	
169						^{152}SmOH	^{153}EuO					^{168}ErH	100		
170						^{154}SmO	^{153}EuOH	^{154}GdO				14.91	^{169}TmH	2.98	
171						^{154}SmOH		^{155}GdO				^{170}ErH		14.09	
172								^{156}GdO		^{156}DyO				21.69	
173								^{157}GdO		^{164}DyOH				16.1	
174								^{158}GdO		^{158}DyO				32.03	
175								^{158}GdOH	^{159}TbO	^{164}DyOH				^{174}YbH	97.4
176								^{160}GdO	^{159}TbOH	^{160}DyO				13	2.6

Figure 2 Isotopes of the lanthanides with abundances [Meija et al, 2016] and their most prominent hydride, oxide and hydroxide interferences in ICP-MS, based on water and nitric acid chemistry. The green marked isotopes are not interfered or only slightly interfered and can be used for quantitative determination. The red marked isotopes should be avoided for quantitative measurements. The yellow marked isotopes are the best choices for the interfered elements and may be used for determination. Barium is included to show the importance of considering this element when measuring the lanthanides. All oxides in the chart refer to $^{16}O^{+}$.

Many ways of avoiding the impact of polyatomic interferences have been proposed. Neutron activation analysis (NAA) is a non-mass spectrometric technique that provides relatively low detection limits but requires access to a research reactor [Bulska et al., 2012; Dampare et al., 2005]. Funderberg et al. [2017] has presented a method for measuring the lanthanide series using medium-resolution LA-ICP-MS (laser ablation ICP-MS) which allows for peak separation of the polyatomic interferences from the analytes. However, the method did not resolve the interference of e.g. $^{143}Nd^{16}O^{+}$ on $^{159}Tb^{+}$. The resolution needed to resolve these peaks is approximately 7700. Using higher resolution also

decreases the sensitivity that may be required to measure low concentrations with good accuracy and precision [Nelms, 2005]. Attempts have been made to correct for these interferences mathematically [Raut et al., 2003; Vaughan and Horlick, 1990] but this approach may lead to large measurement uncertainties if the correction is large compared to the analyte in question and may require extensive measurements each day of analysis [Simitchiev et al., 2008]. Groopman et al. [2017] has presented the SIMS-SSAMS (secondary ion mass spectrometry-single stage accelerator mass spectrometry) as an excellent technique for providing interference free lanthanide patterns at low concentrations. However, this technique is rare and therefore there is a need for more available mass spectrometric techniques. Inductively coupled plasma-mass spectrometry (ICP-MS) is a widespread, multi-elemental technique that is suitable for the purpose due to low detection limits for these elements.

Many papers have put forward the possibility of performing chemical separations for at least some of the elements in the lanthanide series to remove interfering lanthanide oxides. Pin and Zalduegui [1997] used a combination of TRU resin (CMPO/TBP) and Ln resin (HDEHP) to separate thorium and uranium and light rare earth elements, LREE, respectively for measurement of neodymium isotope ratios and concentrations of uranium, thorium, neodymium and samarium. Another example is Yang et al [2010] who presented a separation method using Ln resin for measuring both Sm-Nd and Lu-Hf isotope systems used for geochronological dating.

3.2 MEASUREMENT TECHNIQUES

3.2.1 Gamma spectrometry

Gamma spectrometry is a non-destructive measurement method for gamma emitting radionuclides. The instruments used for gamma spectrometry can be divided into low- and high-resolution instruments. Low-resolution instruments such as NaI(Tl) scintillation detectors [Knoll, 2000] are commonly used as first-responder or customs instruments, but the ability of these instruments to identify radionuclides has been shown to be unsatisfactory [Blackadar et al. 2003; Nelson et al., 2011; Pibida et al., 2004]. This is mainly due to the low-resolution characteristics. A number of publications have put forward different identification algorithms but the problem seems to remain [Estep et al., 1998; Hofstetter et al., 2008; Sprinkle Jr et al., 1997]. The instrument is not able to separate peaks that are close in energy, which makes the instrument a blunt tool for identification and requires highly qualified users in many cases. However, this is not always enough since the resolution often prohibits even manual identification. The instrument used in **Paper I** does have the ability to automatically evaluate both measured nuclides as well as the category regarding uranium. High-resolution instruments, high purity germanium detectors (HPGe) [Knoll, 2000], do not have this problem.

An advantage of low-resolution instruments is that they operate at room temperature as opposed to HPGe detectors that require cooling. The need for cooling in HPGe detectors somewhat limits its flexibility. Another advantage of the low-resolution detectors is that the acquisition is fast due to the high measurement efficiency since e.g. NaI(Tl) detectors can be produced with a much larger volume compared to HPGe detectors.

3.2.1.1 Absolute and relative efficiency calibrations

As the measurement efficiency of a gamma spectrometric system is energy dependent, the detectors need carefully executed efficiency calibrations in order to make accurate activity and activity ratio measurements. This is normally done by using a calibration solution containing a number of radionuclides with known, certified activities and with energies covering the energy region in question.

The radioactivity of isotope x, A_x, evaluated from a gamma spectrometric measurement is given by

$$A_{\mathrm{x}} = \frac{C_{\mathrm{x},\gamma}}{t \cdot I_{\mathrm{x},\gamma} \cdot \Psi_{\gamma}} \tag{3}$$

where $c_{x,\gamma}$ and $I_{x,\gamma}$ are the number of counts and photon emission probability of isotope x at energy E_γ, respectively, t is the measurement time and Ψ_γ is the measurement efficiency at energy E_γ. The measurement efficiency is given by rearranging Eq. 3:

$$\Psi_{\gamma} = \frac{C_{\mathrm{x},\gamma}}{t \cdot I_{\mathrm{x},\gamma} \cdot A_{\mathrm{x}}} \tag{4}$$

Hence, the calibration spectra and the certificate information for each energy can be used to fit a response function by using an empirical equation. In this work the 5-term equation previously published by Ramebäck et al. [2010] where c_1,…, c_5 are constants and E is the energy, has been used:

$$\Psi(E) = e^{c_1 + {c_2}/{E^2} + c_3 \cdot (\ln(E))^2 + c_4 (\ln(E))^3 + {c_5}/{E}} \tag{5}$$

In special cases, where the absolute activity is unimportant, such as in activity or isotope ratio determinations, it is possible to construct a relative calibration if there is a radionuclide in the sample with a number of gamma lines covering the energy region of interest. As the activity is equal for all calibration points, Eq. 4 can be simplified and the relative measurement efficiency for a certain gamma line is then given by

$$\Psi_{\mathrm{rel},\,\gamma} = \frac{C_{\mathrm{x},\gamma}}{I_{\mathrm{x},\gamma}} \tag{6}$$

The calculated $\Psi_{rel,\gamma}$ can be used to fit Eq. 5 in the same manner. The advantage of using inherent calibrations is that the sample geometry including absorbing materials between the sample and the detector as well as sample composition is unimportant as opposed to absolute calibrations. The peaks used for the construction of an intrinsic response function for uranium abundance calculations in high-resolution spectra are peaks in the low energy region for ^{235}U and peaks in the high-energy region for ^{234m}Pa. The condition for fitting the function is that the ^{234m}Pa peak at 258 keV is visible. This peak connects the low energy ^{235}U peaks with the high-energy ^{234m}Pa peaks and enables a fit of a function over the whole energy region, from 144 keV to 1001 keV. For high-resolution instruments, this vital peak is visible in almost all uranium spectra except possibly spectra of very highly enriched uranium. In the case of very highly enriched uranium in the high-resolution case, it would be possible to use ^{228}Th daughters to establish the response function if the material contains reprocessed uranium (^{232}U) [Ramebäck et al., 2010]. However, for low-resolution instruments, this peak is not discernible and, furthermore, the low resolution reduces the number of distinct peaks for the fitting of the response function from eight to two or possibly three peaks. Hence, the construction of an intrinsic response function of a low-resolution spectrum is not possible. Instead, the instrument must be calibrated for absolute efficiency for a certain measurement setup.

3.2.1.2 Categorization of uranium by gamma spectrometry

Uranium can be categorized by evaluating the fraction of ^{235}U of the total amount of uranium. Using gamma spectrometry, this can be done by using the 185.7 keV peak from ^{235}U and the 1001 keV peak from ^{234m}Pa in the gamma spectrum, assuming radioactive equilibrium between ^{234m}Pa and ^{238}U. Four months after separation, the activity difference between ^{234m}Pa and ^{238}U is within the uncertainty of the gamma spectrometric measurement. Hence, radioactive equilibrium can be assumed after this period of time. The abundance of ^{235}U, f_{235}, is, if the abundance of minor uranium isotopes is neglected, given by

$$f_{235} = \frac{N_{235}}{N_{235}+N_{238}} \tag{7}$$

where N_x is the number of atoms of uranium isotope x. When the enrichment of ^{235}U approaches 90%, the ^{234}U abundance is around 1% depending on the history of the material [Nguyen and Zsigrai, 2006]. Therefore, the amount of ^{234}U, N_{234}, is, in this case, considered negligible. Furthermore, the 185.7 keV peak is assumed not to be interfered by ^{226}Ra. This assumption is made on the basis that there are no significant amounts of ^{226}Ra in a processed anthropogenic uranium material due to the relatively young age. Moreover, the ^{226}Ra originating from the background may be subtracted from the spectrum.

Using the well-known relation

$$A_{\mathrm{x}} = \frac{N_{\mathrm{x}} \cdot \ln(2)}{t_{½,\mathrm{x}}} \tag{8}$$

where $t_{½,x}$ is the half-life of isotope x in combination with Eq. 6-7, the abundance of ^{235}U can be written as:

$$f_{235} = \frac{c_{235,185\mathrm{keV}} \cdot t_{½,235} \Big/ I_{235,185\mathrm{keV}} \cdot \Psi_{185\mathrm{keV}}}{c_{235,185\mathrm{keV}} \cdot t_{½,235} \Big/ I_{235,185\mathrm{keV}} \cdot \Psi_{185\mathrm{keV}} + c_{238,1001\mathrm{keV}} \cdot t_{½,238} \Big/ I_{238,1001\mathrm{keV}} \cdot \Psi_{1001\mathrm{keV}}} \tag{9}$$

3.2.2 ICP-MS

The mass spectrometer used in this work is a double focusing sector field ICP-MS, Element 2 (Thermo Scientific, Bremen, Germany). Double focusing means the ions are separated by both mass in a magnetic sector and by energy in an electrostatic analyser (ESA). The ESA may be placed either before or after the magnet sector (Nier-Johnson and reversed Nier-Johnson geometry, respectively). The instrument used in this work has the reversed Nier-Johnson geometry, which improves abundance sensitivity and reduces noise since the mass analyser reduces the high ion currents from the ion source and the only ions that reach the ESA are ions with the correct mass [Jakubowski et al., 1998].

3.2.2.1 Interferences

Interferences in mass spectrometry can be divided into two groups, spectral and non-spectral interferences.

3.2.2.1.1 Polyatomic interferences

Common spectral interferences in mass spectrometry are the polyatomic interferences. These interferences are the result of two or more atoms in the matrix, solvent or plasma gas, forming a molecular species. The formation rate and type of molecule is largely dependent on the presence of isotopes and the plasma conditions [Nelms, 2005]. Common polyatomic species are argides, nitrides, oxides and hydrides due to the abundance of these elements in the plasma and the solvent [Jakubowski et al., 2011]. Due to the dependence on sample composition and plasma conditions, the

amount and type of polyatomic interferences may be difficult to predict, making mathematical interference corrections difficult to perform. One way to remove the interferences is to increase the resolution, but this measure may not be sufficient to remove all interferences [Funderberg et al., 2017].

3.2.2.1.2 Isobars

Many of the isotopes measurable with ICP-MS have isobars, i.e. isotopes of another element but with the same mass, such as $^{241}Pu^{+}$ and $^{241}Am^{+}$. This type of interference requires very high resolution for peak separation (up to 10^{7} [Nelms, 2005]). Therefore, the options when measuring these isotopes are to either correct for the interference or remove the elements with interfering isotopes using chemical separations. Since the isobars in many cases are predictable it is possible to mathematically subtract the portion of the peak coming from the interfering isotope, assuming that the elements have a natural composition [Jakubowski et al., 2011].

3.2.2.1.3 Multiply charged ions

Multiply charged ions arise when the atom loses more than one electron in the plasma. The detection of the formed ion will be at mass m/Z where Z is the charge of the ion. The probability of the formation of multiply charged ions is low since the second ionisation energy is substantially higher than the first ionisation energy but can cause interference problems if the interfering element is abundant in the measured samples. One such example is the measurement of trace lanthanides in a uranium matrix where ^{139}La may be interfered by $^{238}U^{40}Ar^{++}$ [Boulyga et al., 2017].

3.2.2.1.4 Abundance sensitivity

A fourth kind of spectral interference is the tailing of isotopes on neighbouring masses. Due to scattering of ions in the beam, the energy spread of the ions increases, resulting in higher abundance sensitivity [Becker, 2007]. A typical abundance sensitivity is between 10^{-7}-10^{-6} [Nelms, 2005]. Therefore, the abundance sensitivity does not affect the measurement unless the ratio between the tailing isotope and the neighbouring isotope is >100000 [Nelms, 2005].

3.2.2.1.5 Non-spectral interferences

Non-spectral interferences, or matrix effects, are effects that are not limited to a certain mass but cause an overall change in the analyte signal independent of the mass [Evans and Giglio, 1993; Nelms, 2005]. The signal changes are caused by for example sample transport, ionization in the plasma and ion extraction. Another reason for signal suppression may be build-up of salts on the cones causing the orifices to clog [Evans and Giglio, 1993]. The level of the matrix effect depends on the concentration and nature of the matrix. A heavy matrix often leads to signal suppression and can be resolved by dilution or, to some extent, the use of an internal standard. Another way to minimize matrix effects is to chemically separate the analytes from matrix elements.

Corrections for non-spectral interferences can be done by the use of an internal standard. The internal standard should be an element absent in the sample and show the same behaviour as the analyte in the plasma. It has been suggested that elements suitable as internal standards have mass and ionization potential close to the analyte [Thompson and Houk, 1987]. According to Vanhaecke et al. [1992], only the mass needs to be a close match for the internal standard to be appropriate. In this study, the impact of ionization potential was regarded as insignificant.

3.2.2.2 Quantification

For quantification, different approaches such as isotope dilution, standard addition and external calibration, can be used.

3.2.2.2.1 Isotope dilution

The approach that usually provides the lowest measurement uncertainties is isotope dilution, where a spike with a different isotopic composition than the isotopic composition of the analyte in the sample, is added to the measured sample [Trešel et al., 2003]. Another possibility is to use an isotope, which is not naturally occurring, i.e. long-lived radioactive isotopes. One such example is the use of ^{233}U for quantification of uranium [Kristo et al., 2015, Nelwamondo et al., 2018]. By knowing the isotopic compositions of the spike and the sample as well as the amount of added spike, the concentration of the sample can be determined. A limitation to this method is the lack of reference materials that are isotopically enriched to be useful for isotope dilution. Another limitation is that some elements, such as aluminium and yttrium, have only one stable isotope, which makes isotope dilution impossible.

3.2.2.2.2 Standard addition

In standard addition, increasing and known amounts of the analyte is added to the sample and by measuring the sample with an increasing amount of analyte spike, it is possible to calculate the amount of the analyte in the sample when no spike is added as the relation between signal intensity and the concentration is linear [Harris, 2003]. Standard addition limits the impact of matrix effects but may require tedious work, as every measured sample requires a number of measurements with different amounts of analyte spike.

3.2.2.2.3 External calibration

Due to the lack of isotopic spikes and the work effort of standard addition, the most commonly used method for quantitative measurements by ICP-MS is done using external calibration where calibration samples with a known amount of analyte are measured to establish a calibration with instrument signal as a function of concentration [Nelms, 2005]. In this way, unknown samples can be measured and the signal from the sample can be used to calculate the concentration. External calibrations using pure standard solutions do not take any matrix effects into account. Depending on the matrix, analyte concentrations in the sample can be over- or underestimated. Therefore, the calibration samples often need to be matrix-matched when the samples have a high matrix content, in order to provide a calibration that corresponds to the samples [Nelms, 2005].

3.3 SEPARATION CHEMISTRY

3.3.1 Solvent extraction

The purpose of solvent extraction may be to preconcentrate the analyte(s), eliminate matrix interferences or to differentiate chemical species, and is a method to separate compounds depending on differentiating solubility in two immiscible phases, normally an aqueous phase and an organic phase. The distribution ratio, *D*, of a compound between the organic phase and the water phase can be expressed by:

$$D = \frac{[M]_{org}}{[M]_{aq}} \tag{10}$$

where $[M]_{org}$ and $[M]_{aq}$ is the total concentration, i.e. the concentration of all species of M, in the organic and aqueous phase, respectively [Nash, 2000]. The organic phase consists of an extractant that has the ability to extract the desired compound from the aqueous phase into the organic phase, i.e. making it more soluble in the organic phase. Sometimes a diluent is added to enhance the performance of the extractant. The goal of the extraction is to form an uncharged hydrophobic molecule that includes the wanted species, which can be dissolved in the organic phase.

The extractants can be divided into different groups depending on the extraction mechanism [Rydberg, 1992]. Some examples of extractants and their mechanisms are acidic extractants, basic or ion pair forming extractants and solvating or neutral extractants. The overall mechanism for acidic extractants, where the metal cation reacts with a suitable anion, the extractant, to form a neutral complex, can be written as

$$M^{n+} + \overline{nHA} \rightleftharpoons \overline{MA_n} + nH^+ \tag{11}$$

The ion pair forming extractant mechanism where the metal cation forms an ion pair with the extractant can be summarized as

$$MX_p^{(n-p)-} + \overline{(n-p)R_3NH^+X^-} \rightleftharpoons \overline{R_3NH_{(n-p)}MX_p} + (n-p)X^- \tag{12}$$

Correspondingly, the mechanism of solvating extractants where the coordinated water molecules are replaced by an organic solvating reagent can be written as

$$MY_q + \overline{rB} \rightleftharpoons \overline{MY_qB_r} + xH_2O \tag{13}$$

The species in reactions 11-13 with a line on top are species in the organic phase. In this work, commercial resins, Ln resin (Triskem, Bruz, France) based on di-2 ethylhexyl orthophosphoric acid (HDEHP) have been used.

3.3.2 Extraction using HDEHP

HDEHP, see Figure 3, has for a long time been used for the separation of lanthanides and other trivalent elements and the properties of the HDEHP extractant system has been thoroughly investigated [Qureshi et al., 1969; Alstad et al., 1974; Peppard et al., 1957].

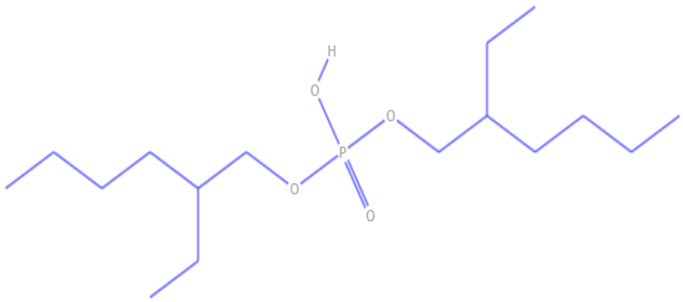

Figure 3. Structural formula of HDEHP.

The overall reaction is assumed to be:

$$M^{3+} + \overline{3(HDEHP)_2} \rightleftharpoons \overline{M(H(DEHP)_2)_3} + 3H^+ \quad (14)$$

where M^{3+} is the lanthanide ion [Alstad et al, 1974]. Peppard et al. [1957] showed that the extraction of the lanthanides show an inverse third-power dependence on the acid concentration which agrees with Eq. 14, and if the acid concentration increases, the extraction decreases, allowing for stripping of the extracted species. However, Alstad et al. [1974] showed that this dependence becomes directly proportional at nitric acid concentrations above approximately 5 M. Qureshi et al. [1969] proposed two possible mechanisms for this increased extraction:

$$M^{3+} + 3X^- + \overline{(HDEHP)_2} \rightleftharpoons \overline{MX_3(HDEHP)_2} \quad (15)$$

$$H^+ + X^- + \overline{(HDEHP)_2} \rightleftharpoons \overline{HX(HDEHP)_2} \quad (16)$$

where X^- represents the anion of the acid. The proposed reaction in Eq. 15 indicates that increasing the amount of acid anion drives the extraction of the lanthanide to an HDEHP complex together with the anion, while Eq. 16 indicates that acid ions are removed from the aqueous phase that in turn leads to increased extraction of lanthanide ions according to Eq. 14.

3.4 LINEAR REGRESSION

Using external calibration in ICP-MS measurements involves the procedure of fitting a straight line to a number of calibration points with the analytical signal, *y*, as a function of concentration, *x*:

$$y = a + bx \quad (17)$$

where *a* and *b* are the estimates of intercept and slope of the line, respectively. The common method to evaluate this line is to use ordinary least squares regression (OLS) where the distance between the data points and the line along the *y*-axis is minimized [Miller and Miller, 2010]. The slope, *b*, is calculated according to Eq. 18.

$$b = \frac{\sum_i [(x_i - \bar{x})(y_i - \bar{y})]}{\sum_i (x_i - \bar{x})^2} \quad (18)$$

where y_i and x_i are the signal intensity and the concentration of calibration point i, respectively, and $\bar{y}$ and $\bar{x}$ are the corresponding mean values of all calibration points. The intercept can then be calculated by Eq. 19:

$$a = \bar{y} - b\bar{x} \quad (19)$$

However, in order for the OLS to be a valid method for establishing this line, a number of requirements need to be fulfilled [Raposo, 2016; Hubaux and Vos, 1970]:

- A linear relationship between x and y.
- The uncertainty of the concentrations on the x-axis is negligible.
- The variance in y is homoscedastic.
- Normally distributed variance in y.

If at least one of these requirements are not fulfilled, the OLS will not provide the best estimate of the calibration line. Whereas the first and last point frequently are fulfilled in mass spectrometric measurements, the second point at least needs to be evaluated to check the validity of the OLS. However, the third point is almost exclusively invalid in mass spectrometry [Ketkar and Bzik, 2000]. In the case of mass spectrometry, the data points have heteroscedastic variance; the relative variance is the same with the exception of low measurement intensities where the relative variance is higher. Therefore, OLS is not a valid method for fitting a line to mass spectrometric calibration data. In OLS, each data point is given the same importance in the regression, which infers that, even though data points on the far right side of the calibration have higher absolute uncertainties, these data points have unreasonably large impact on the fitted line. This means that at low concentrations, the line does not represent the data points very well.

To fit a line to heteroscedastic data another regression type such as weighted linear regression (WLS) should be used [Sayago, 2004]. In WLS, each data point is weighted with a suitable parameter, or weight factor, to give data points with low absolute variance higher importance in the regression. The classical approach is to use $1/s_y^2$ as weight factor, where s_y is the uncertainty in y [Deming, 1964] but also other weight factors such as $1/y$ or $1/x$ can be used if there is only one data point for each x [Almeida, 2002]. In WLS the slope, b, is calculated as

$$b = \frac{\sum_i w_i [(x_i - \bar{x}_w)(y_i - \bar{y}_w)]}{\sum_i w_i (x_i - \bar{x}_w)^2} \quad (20)$$

where w_i is the weight factor at calibration point i and $\bar{y}_w$ and $\bar{x}_w$ are the weighted mean values of all y_i and x_i. The intercept, a, can be calculated in a corresponding manner to Eq. 19 with the exception that the weighted means of all calibration points are used rather than the means of x and y [Sayago and Asuero, 2004]:

$$a = \bar{y}_w - b\bar{x}_w \quad (21)$$

The detection limit, L_D, used for external calibrations in this thesis is

$$L_D = a + 3u_a \quad (22)$$

where u_a is the uncertainty of the intercept [Miller and Miller, 2010].

4 EXPERIMENTAL

4.1 MEASUREMENT UNCERTAINTY

The measurement uncertainties presented in this work were evaluated according to ISO: Guide to the Expression of Uncertainty in Measurement, ISO/GUM [2008]. The results were calculated using GUM Workbench 2.4 (Metrodata GmbH, Grenzach-Wyhlen, Germany) and are presented with a coverage factor *k*=2, unless otherwise stated which corresponds to an approximate 95% confidence interval.

4.2 LOW-RESOLUTION GAMMA SPECTROMETRY FOR URANIUM CATEGORIZATION

4.2.1 Measurements

Spectra were acquired of the following materials using the hand-held NaI(Tl) scintillation detector identiFINDER (ICx, FLIR Systems Inc., Wilsonville, USA):

- Natural uranium as UO_2
- Low-enriched uranium with an approximately 4% enrichment as UO_2
- Depleted uranium as UO_2
- Natural uranium in an aqueous solution (IRMM-184, Geel, Belgium)

Data was collected for 60 s at a distance of 10 cm from the source. The data from the certified reference material IRMM-184 was collected during 600 s due to low uranium content. The instrument reported the uranium category after the measurement using the automatic evaluation algorithm. The spectrum data was also downloaded for off-line evaluations according to Eq. 5 and Eq. 9.

4.2.2 Simulations

The following setups were simulated using the Monte Carlo based simulation software VGSL (Visual Gamma Spectroscopy Laboratory:

- Water matrix, ρ = 1 g/cm^3
- UO_2 matrix, ρ = 11 g/cm^3
- Uranium metal matrix, ρ = 19 g/cm^3
- Water matrix with a 1 mm lead shielding, ρ_{Pb} = 11 g/cm^3
- Water matrix with a 5 mm steel shielding, ρ_{Steel} = 7.5 g/cm^3

VGSL uses a modified version of MCNPX as particle transport simulation engine [Plenteda, 2002; Waters, 2002]. The detector was simulated to correspond to the identiFINDER. Therefore, the crystal dimensions and density were set to 35 x 51 mm^2 and 3.7 g/cm^3, respectively. Eq. 5 was fitted to each set of efficiency data retrieved from the simulations and the abundance of ^{235}U according to Eq. 9 was calculated for each spectrum, with different response functions, from the peak areas at 185.7 keV and 1001 keV.

4.3 SIGNATURES IN ^{241}AM SOURCES

Five sources were studied for investigation of possible signatures:

- Source 1: ^{241}Am sealed source contained in a lead shield during the gamma spectrometric measurement. Nominal activity 185 GBq.
- Source 2: ^{241}Am sealed source contained in a lead shield during the gamma spectrometric measurement. Nominal activity 185 GBq.
- Source 3: ^{241}Am sealed source measured with 1.1 mm Cd shielding.
- Source 4: Electroplated ^{241}Am source. Nominal activity 3.7 GBq.
- Source 5: Ionising smoke detector containing an ^{241}Am source.

Source 1 and 2 were visually similar. Sources 1-4 were measured overnight, at a distance of about 30 cm using a p-type coaxial high purity germanium detector (Detective-EX, EG&G Ortec, Oak Ridge, TN, USA) which has a relative efficiency of about 15% and a resolution of 2.5 keV at 1332 keV. The smoke detector, Source 5, was measured in a lead shield setup, using a p-type coaxial HPGe detector (EG&G Ortec, Oak Ridge, TN, USA) with a relative efficiency of 50% and a resolution of 2.0 keV at 1332 keV. The measurement time for Source 5 was approximately 1 week due to low activity of its daughter radionuclides.

An intrinsic response function was established for each spectrum using ^{241}Am lines between 59.5 and 801.9 keV, see Table 2, and Eq.5. Using the response function, the activity of ^{233}Pa relative to ^{241}Am could be calculated and the ages of the sources could then be determined using Eq.2. The gamma lines used for the calculation was the 322.6 keV ^{241}Am line and 311.9 keV ^{233}Pa line. Furthermore, the relative activities of the impurity elements could be determined.

Table 2 Gamma energies with corresponding photon emission probabilities used for the intrinsic calibration and the age determination. Data are taken from Decay Data Evaluation Project [2018].

	E_γ [keV]	I_γ [%]
^{241}Am	59.5	35.92
^{241}Am	103.0	0.0195
^{241}Am	125.3	0.0041
^{241}Am	208.0	0.000786
^{233}Pa	300.1	6.6
^{233}Pa	311.9	38.3
^{241}Am	322.6	0.000151
^{233}Pa	340.5	4.47
^{241}Am	376.7	0.000137
^{241}Am	383.8	0.0000281
^{233}Pa	398.5	1.408
^{241}Am	619.0	0.000060
^{241}Am	662.4	0.000367
^{241}Am	722.0	0.000196
^{241}Am	801.9	0.0000012

4.4 LANTHANIDE PATTERN MEASUREMENTS

Two reference materials were used for the study, REE-2 and CUP-2 (both CanmetMINING, Ottawa, Canada). REE-2 is certified for most lanthanides and has provisional values for the lanthanides that are not certified (includes gadolinium, ytterbium and lutetium). CUP-2 is a UOC and is not certified for lanthanides but is often used as a working reference material for lanthanide pattern measurements. The materials were dissolved by microwave digestion and lithium borate fusion, respectively. The samples were measured directly, after an appropriate dilution, using both a standard sample introduction system and a desolvating sample introduction system to study the difference in oxide formation and impact on polyatomic interferences on the elements in the lanthanide series. The samples were also measured after chemical separation where the samples were separated into three different fractions as a measure to avoid interferences.

4.4.1 Oxide formation measurements

To study the lanthanide oxide formation rate, single element standard solutions of each element in the lanthanide series, were diluted to 1 ng g^{-1}, 10 ng $g^{-1}$and 100 ng g^{-1}. Each solution was measured with respect to all masses between 137 and 192 using an ElementXR (Thermo Fischer Scientific, Bremen, Germany) in triple detection mode (counting mode, analog mode and Faraday cup). The sample introduction consisted of a Twinnabar spray chamber and a Micromist nebulizer (both from GlassExpansion, Port Melbourne, Australia). The measurement data was corrected for dead time and blank subtracted. The ratios for each oxide, hydride and hydroxide was calculated.

4.4.2 Sample dissolution

CUP-2 was dissolved by microwave digestion (Mars5, CEM Corporation, Matthews, U.S). 0.2 g of the material was mixed with 9 mL concentrated HNO3 + 0.09 M HF and 1 mL of ultra-pure water (Milli-Q, Merck KGaA, Darmstadt, Germany) in a Teflon tube. The temperature was ramped to 180°C during 20 minutes and that temperature was held for 15 minutes. The samples were thereafter diluted to a concentration of approximately 10 mg U g^{-1}.

The reason for using lithium borate fusion for the REE-2 material was due to incomplete digestion when using the microwave oven. 1 g of the material was placed in a graphite crucible together with 3 g of $LiBO_2$ (Ultrapure, Claisse, Quebec, Canada). The sample was pre-oxidized for 2 h in 650°C. Thereafter, the temperature was increased to 1050°C and the sample was fused for 15 minutes. After cooling, the resulting glass bead was dissolved in 100 mL 1.4 M HNO_3 while heating and stirring. After dissolution, 0.4 g of polyethylene glycol (PEG-2000, Alfa Aesar, Karlsruhe, Germany) was added to flocculate silica. The solution was evaporated to approximately 50 mL and left overnight to let the slow flocculation proceed. The solution was filtered through a OOM filter paper (Munktell, Alstrom Munksjö, Helsinki, Finland) and diluted in 1 M HNO_3. Blanks were prepared in the same manner as the samples for each of the methods above.

4.4.3 Chemical separations

An aliquot was taken from the dissolved reference materials and either diluted to 0.05 M HNO_3 or evaporated to almost dryness and dissolved in 2 mL 0.05 M HNO_3. For the yield determination, two samples were prepared for each replicate whereof one was spiked with a known amount of lanthanide standard solution. Due to the low amount of uranium in the REE-2 reference material, 1 mg of uranium was added to these samples to mimic a high uranium content. The in-house prepared 2 mL Ln resin columns (resin and columns both from Triskem International, Bruz, France) were conditioned with 1 mL 0.05 M HNO_3. Thereafter, the samples were added to the column. The samples tubes were rinsed with 2x1 ml 0.05 M HNO_3 and the rinse solutions were also added to the columns. Next, La-Nd was eluted into 25 mL Teflon beakers using 6 mL 0.4 M HCl. The beakers were changed and Sm-Gd was eluted with 10 mL 0.75 mL HCl. The change of beakers was repeated and Tb-Lu was eluted using 20 ml 10 M HNO_3. All solutions were evaporated to near dryness and dissolved in 2% nitric acid.

4.4.4 Measurements

The unseparated samples as well as the separated samples were diluted to a concentration between 6 pg g^{-1} and 2 ng g^{-1} using 2% HNO_3. Indium, rhodium and rhenium was added as internal standard to a concentration of 1 ng g^{-1}. The choice of internal standard element depended on lanthanide.

The measurements were performed on an Element2 (Thermo Fischer Scientific, Bremen, Germany). The standard sample introduction consisted of a cyclonic Twister spray chamber and a 1 mL min^{-1} concentric Conikal nebulizer (both from GlassExpansion, Port Melbourne, Australia). The desolvating sample introduction system consisted of a Cetac Aridus II and a 100 µL min^{-1} C-flow nebulizer (both from Teledyne Cetac Technologies, Omaha, Nebraska, US). The instrumental settings and measurement parameters can be found in Table 3. The instrument was tuned with a 1 ng g^{-1} cerium standard solution to minimize the cerium oxide formation rate and maximizing the sensitivity.

Table 3 Instrumental settings for the two sample introduction systems measurement parameters.

	Standard sample introduction	**Desolvating sample introduction**
	Twister spray chamber	**Aridus II**
Nebulizer	Conikal	C-flow PFA
Forward power [W]	1250	1200
Cool gas flow [L min^{-1}]	16	16
Auxiliary gas flow [L min^{-1}]	0.7	0.7
Nebulizer gas flow [L min^{-1}]	1.1	0.9
Ar Sweep gas [L min^{-1}]	N/A	3.2
Nitrogen [mL min^{-1}]	N/A	10
Resolution	300	
Mass window	5%	
Samples per peak	100	
Runs and passes	100 x 1	
Scan type	E-scan	
Measured analyte isotopes	^{137}Ba, ^{139}La, ^{140}Ce, ^{141}Pr, ^{146}Nd, ^{147}Sm, ^{153}Eu, ^{157}Gd, ^{159}Tb, ^{163}Dy, ^{165}Ho, ^{167}Er, ^{169}Tm, ^{174}Yb, ^{175}Lu	
Measured internal standard isotopes	^{103}Rh, ^{115}In, ^{185}Re	

The quantification was performed with a calibration curve based on five points using standard solutions certified by mass. For the direct measurements, a multi-element solution containing all lanthanides (Sigma Aldrich, Buchs, Switzerland) was used. For the separated samples, three different certified standard solutions containing La-Nd, Sm-Gd and Tb-Lu, respectively (Spectrascan, Inorganic Ventures, Christiansburg, USA) were used. For quality assurance, a control sample consisting of a dilution of a certified standard solution of different origin than the calibration standard solution was used (CPAchem Ltd, Stara Zagora, Bulgaria). For the direct measurements, the control sample standard solution was purchased from Sigma Aldrich (Buchs, Switzerland) and for the separated samples, the standard solutions were purchased from CPAchem Ltd (Stara Zagora, Bulgaria).

The dead time was evaluated according to Appelblad and Baxter [2000] using a Lu standard solution. All data reduction and calculations were performed off-line. The external calibrations, using weighted linear regression with the standard uncertainty in *y* as weight, were carried out according to Sayago and Asuero [2004] and the calculations as well as the measurement uncertainties were evaluated using a Monte Carlo method in the same manner as Ramebäck and Lindgren [2018] using Microsoft Excel. The measurement results were normalized with respect to Chondrite values, see Figure 10-11 and 13-14 [Anders and Grevesse, 1989].

4.5 EXTERNAL CALIBRATION FOR TRACE ELEMENT ANALYSIS

4.5.1 Sample preparation

Three different certified reference materials (CRM) were chosen for the study: Periodic Table Mix 3 for ICP (Sigma Aldrich, Buchs, Switzerland), Spectrascan (Spectrascan, Inorganic Ventures, Christiansburg, USA) and CPAchem (CPAchem Ltd, Stara Zagora, Bulgaria). All reference materials were certified by mass and traceable to NIST. The certified uncertainty varied between 0.2% and 0.8% depending on analyte and supplier. One of the CRMs was used as a calibration standard and was diluted to 500 pg g^{-1}, 1000 pg g^{-1}, 1500 pg g^{-1}, 2000 pg g^{-1} and 2500 pg g^{-1}. The other two CRMs were used as quality control samples and diluted to 100 pg g^{-1} and 1000 pg g^{-1}. The dilutions were performed using in-house sub-boiled nitric acid and ultra-pure water. All measurement samples contained 2% HNO_3. 1 ng g^{-1} rhodium was added to each sample as internal standard. Blank samples were prepared together with the samples. The sample preparation was performed gravimetrically in order to reduce uncertainties compared to volumetric additions. However, uncertainty modelling was also done in order to compare volumetric and gravimetric additions from an uncertainty perspective. The analytical balance used in this work was a Mettler Toledo AX204 (Columbus, Ohio, US) with an uncertainty of 0.3 mg, *k*=2.

4.5.2 Measurements

The measurements were performed using an Element 2 (Thermo Scientific, Bremen, Germany) with a concentric nebulizer and a cyclonic spray chamber (both GlassExpansion, Melbourne, Australia). The conditions for the measurement setup can be found in Table 3. Also in this case, the instrument was tuned with a 1 ng g^{-1} cerium solution to maximize the signal of cerium while keeping the formation of CeO low. The magnitude of the CeO formation was 2.5% during all measurements.

4.5.3 Data evaluation

All measurement raw data from calibration and quality control samples were extracted from the instrument software and evaluated offline. For each sample, the mean intensity and standard deviation of the mean were calculated from the 500 data points resulting from samples per peak and 100 sweeps, for each isotope. The intensities were corrected for dead time and thereafter corrected for internal standard. The internal standard intensities were corrected for the added amount of internal standard according to Eq. 23 to improve the internal standard correction:

$$I_{corr,i,j} = \frac{I_{i,j}}{\frac{I_{IS,i}}{m_{IS,i}}} * \frac{I_{IS,blk}}{m_{IS,blk}} \quad (23)$$

where $I_{corr,i,j}$ is the intensity for isotope *j* in sample *i* corrected for internal standard, $I_{i,j}$ is the dead-time corrected intensity of isotope *j* in sample *i*, $I_{IS,i}$ and $I_{IS,blk}$ are the dead-time corrected intensities of the internal standard in sample *i* and the blank sample and $m_{IS,i}$ and $m_{IS,blk}$ are the mass of the added internal standard in sample *i* and the blank sample, respectively. Calibration functions were calculated using two methods, OLS and WLS with the standard uncertainty in *y* as weight, see Eqs. 18-19 and Eqs. 20-21, respectively. OLS was performed using the LINEST() function in Microsoft Excel 2016. In the OLS regression, additional regression statistics was retrieved and used as uncertainties. Using WLS, two different regressions were calculated using uncertainties from sample preparations performed gravimetrically as well as volumetrically to compare the differences in the results depending on choice of sample preparation. For each type of linear regression, the slope and intercept together with uncertainties of respective parameter were estimated.

The calibration functions were used to calculate the detection limits according to Eq. 22 and to evaluate the concentrations of the quality control samples of the two CRMs here named Standard solution 1 and 2. The calculated concentrations were compared to the certified value using the zeta score (ζ) [ISO 13528:2015]:

$$\zeta = \frac{c_{measured} - c_{reference}}{\sqrt{u^2(c_{measured}) - u^2(c_{reference})}} \quad (24)$$

where $c_{measured}$ is the measured and calculated concentration and $c_{reference}$ is the certified concentration and $u(c_{measured})$ and $u(c_{reference})$ are their respective uncertainties. If $|\zeta| \leq 2$ the measured value is consistent with the certified value within their respective uncertainties at a 95% confidence level.

5 RESULTS AND DISCUSSION

5.1 LOW-RESOLUTION GAMMA SPECTROMETRY FOR URANIUM CATEGORIZATION

The fitted simulated response functions can be seen in Figure 4. It is obvious that the response of a very dense material such as uranium metal is very different from the response of a matrix containing water. This effect is seen in both the low as well as the high-energy region but is more prominent in the low energy region. The efficiency at 185.7 keV is approximately 40 times higher in the water matrix than in the uranium metal matrix. At 1001 keV, the difference is a factor 2.9. It is evident that the enrichment calculation of a water sample using a response function for a uranium metal matrix will overestimate the enrichment.

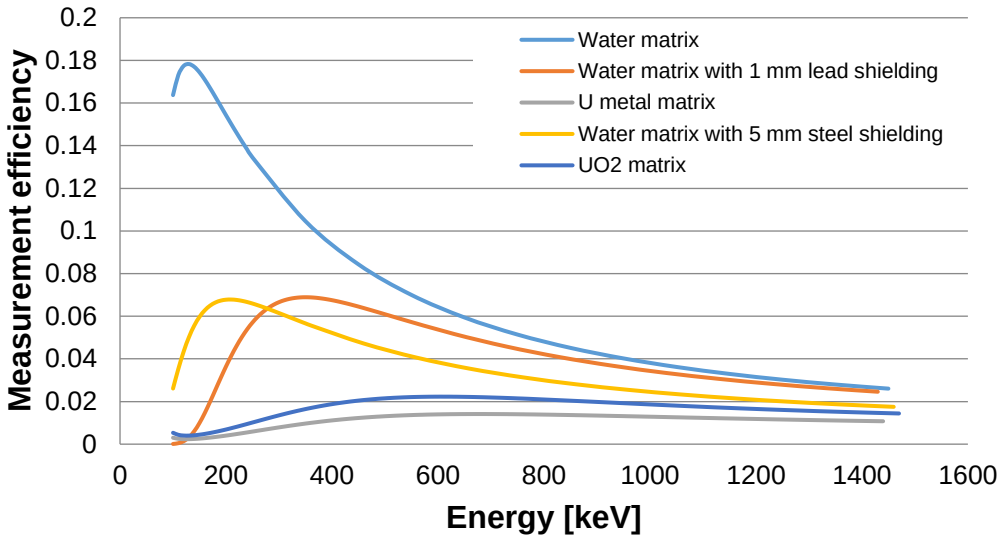

Figure 4 Simulated response functions for the investigated matrices and shielding.

The results of the categorizations done by the Identifinder can be found in Table 4. The table shows that UO_2 is categorized as depleted uranium (DU) independent of the enrichment for the measured materials. On the other hand, the natural uranium (NU) water sample is categorized as low-enriched uranium (LEU). This implies that the response function used in the instrument is based on neither UO2 nor a water matrix.

Table 4 Results of the automatic instrument categorization.

Uranium type	Sample matrix	Instrument categorization
NU	UO_2	DU
LEU	UO_2	DU
DU	UO_2	DU
NU	Aqueous	LEU

The American National Standard Performance Criteria for Hand-Held Instruments for the Detection and Identification of Radionuclides states that an instrument should be able to identify radionuclides shielded by 5 mm of steel [ANSI N42.34-2006]. The results of the evaluated enrichment of all collected spectra using all response functions can be seen in Table 5. The results show that when the correct

response functions are used, i.e. the UO_2 matrix response function for the UO_2 samples and the water matrix response function for the aqueous sample, the enrichments agree with the materials.

Table 5 Results from enrichment calculations using all simulated response functions, respectively.

Sample		**Evaluated abundance of ^{235}U, f_{235}, with respective response function**				
Uranium type	**Real matrix**	**Water matrix**	**Water matrix + 5 mm steel shielding**	**Water matrix + 1 mm lead shielding**	**UO2 matrix**	**U metal matrix**
NU	UO_2	0.000681(51)	0.001052(79)	0.00348(26)	0.00882(66)	0.01041(78)
LEU	UO_2	0.00166(20)	0.00257(30)	0.0085(10)	0.0213(25)	0.0251(30)
DU	UO_2	0.0000449(63)	0.000069(10)	0.000230(32)	0.000587(82)	0.00069(10)
NU	Aqueous	0.0106(16)	0.0163(24)	0.0520(77)	0.123(18)	0.142(21)

On the other hand, the instrument categorization results agree well with the results obtained using the water matrix + 5 mm steel shielding response function. This implies that the inherent response function of the instrument could be based on a water matrix with a 5 mm steel shielding, or something similar.

The results show that it is evident that a correct categorization requires knowledge of the investigated material. If the categorization algorithm is dependent of the nature of the uranium material, which seems to be the case with this instrument, the outcome of the instrument is unreliable. It is therefore necessary for the user to take the acquired spectrum off-line and perform enrichment calculations using response functions based on the knowledge of the material to make sure that the categorization is accurate.

To solve the problem with misclassifications, one option could be to provide the instrument with a range of response functions covering a variety of matrices. The user could then select the appropriate response function depending on the nature of the investigated material, when this is known. If the composition of the material is unknown, the evaluation could be performed with a number of response functions to provide a range of categories for initial decision-making.

5.2 SIGNATURES IN ^{241}AM SOURCES

The fitted response function using the ^{241}Am peaks for Source 1 can be seen in Figure 5.

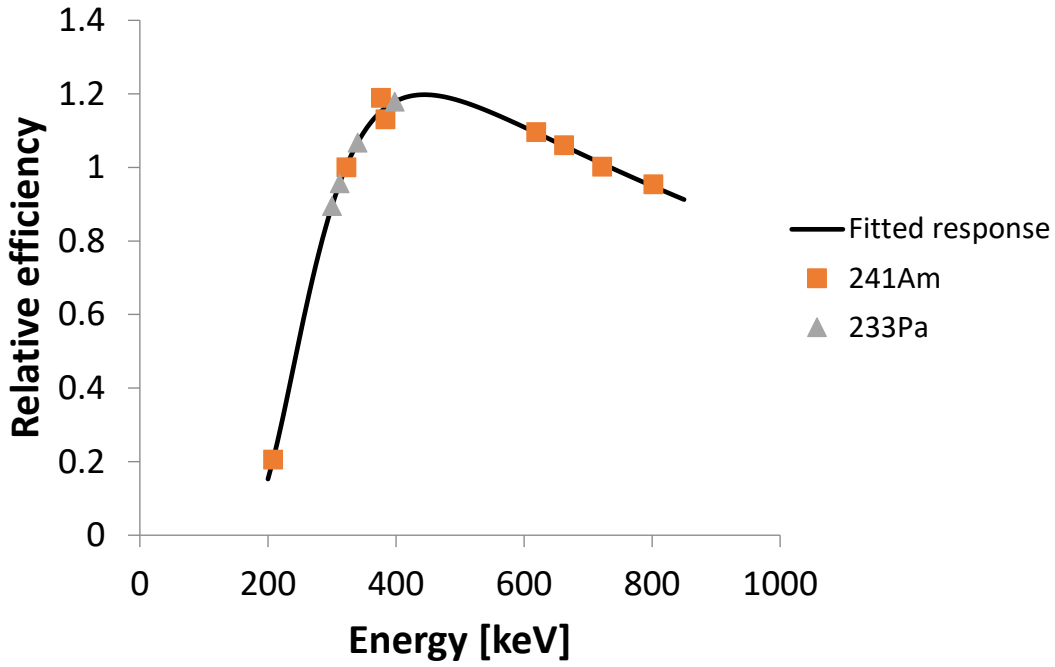

Figure 5 Efficiency response function of Source 1. The squares are the ^{241}Am gamma lines used for the response function construction and the triangles are calculated responses for ^{233}Pa peaks.

5.2.1 Age

The calculated ages at the time of measurement as well as the corresponding separation dates of all sources can be found in Table 6. The results show that Source 1 and Source 2, which are visually similar, have significantly different ages. The age of Source 4 was known, since the chemical separation and the electroplating was performed in 2001, which is in very good agreement with the calculated age.

Table 6 Results for the age determination of the different sources. The presented ages are the ages at the time of measurement. The separation dates are derived from the calculated ages at the time of measurement.

	Age [y]	U [y] *k*=2	Separation date
Source 1	31.4	2.0	1982-01-06
Source 2	40.8	2.6	1972-07-18
Source 3	43.9	3.6	1969-07-06
Source 4	12.2	2.3	2001-06-25
Source 5	21.5	6.9	1985-07-09

5.2.2 Impurities

Spectra from Source 1-3 show peaks at gamma lines that do not originate from ^{241}Am. Many of these peaks do not have a Gaussian shape. Instead, they seem to have two components, a narrow top and a broad base. The broad base is explained by Doppler broadening which occurs when an atom captures a particle and the formed nucleus de-excites while still in motion [Gilmore, 2008]. A comparison between a normal-shaped, Gaussian peak and a Doppler broadened peak can be seen in Figure 6.

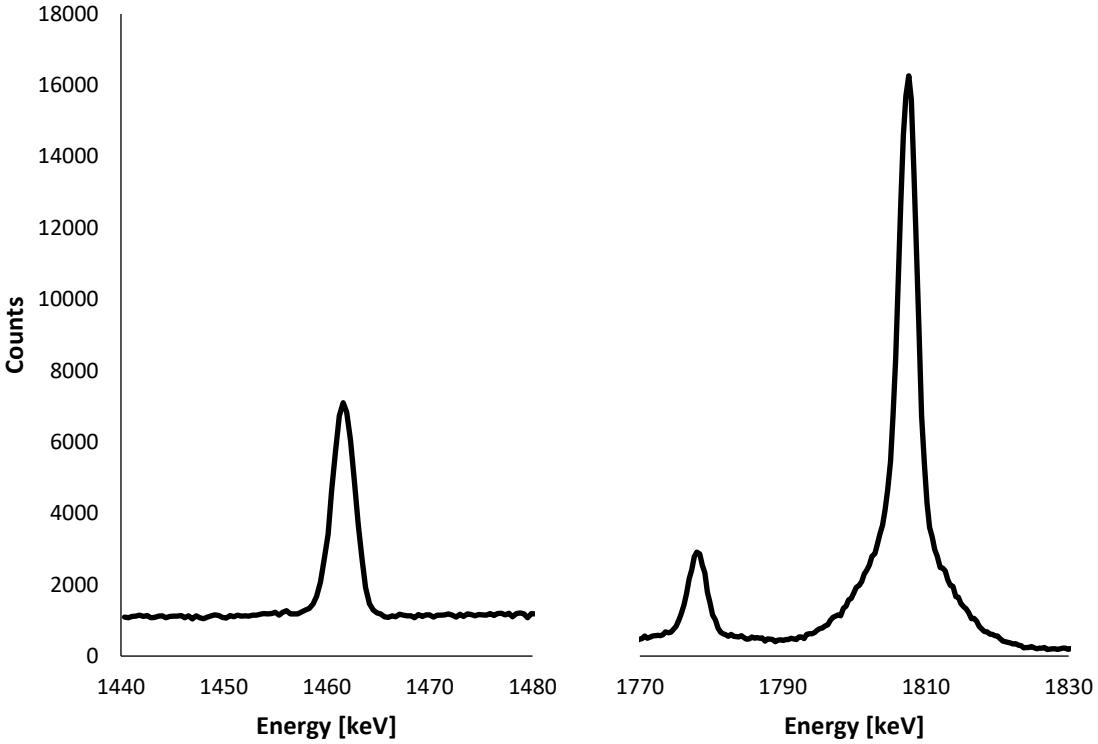

Figure 6 Left: Gaussian 1460 keV peak of ^{40}K, right: a peak, which is Doppler, broadened at the base.

This type of reactions (capture of alpha particles, neutrons or protons) requires that low-Z elements are present in the source to be more probable. Therefore, these peaks indicate that there are low-Z elements present in the sources and that nuclear reactions are taking place within the sources [Gehrke et al., 2003; Catz and Amiel, 1967]. Proposed reactions and their corresponding gamma peaks found in spectra from Source 1-3 can be seen in Figure 7. Source 4 and 5 are ^{241}Am electroplated on stainless steel. Therefore, there are no signs of low-Z elements in these spectra.

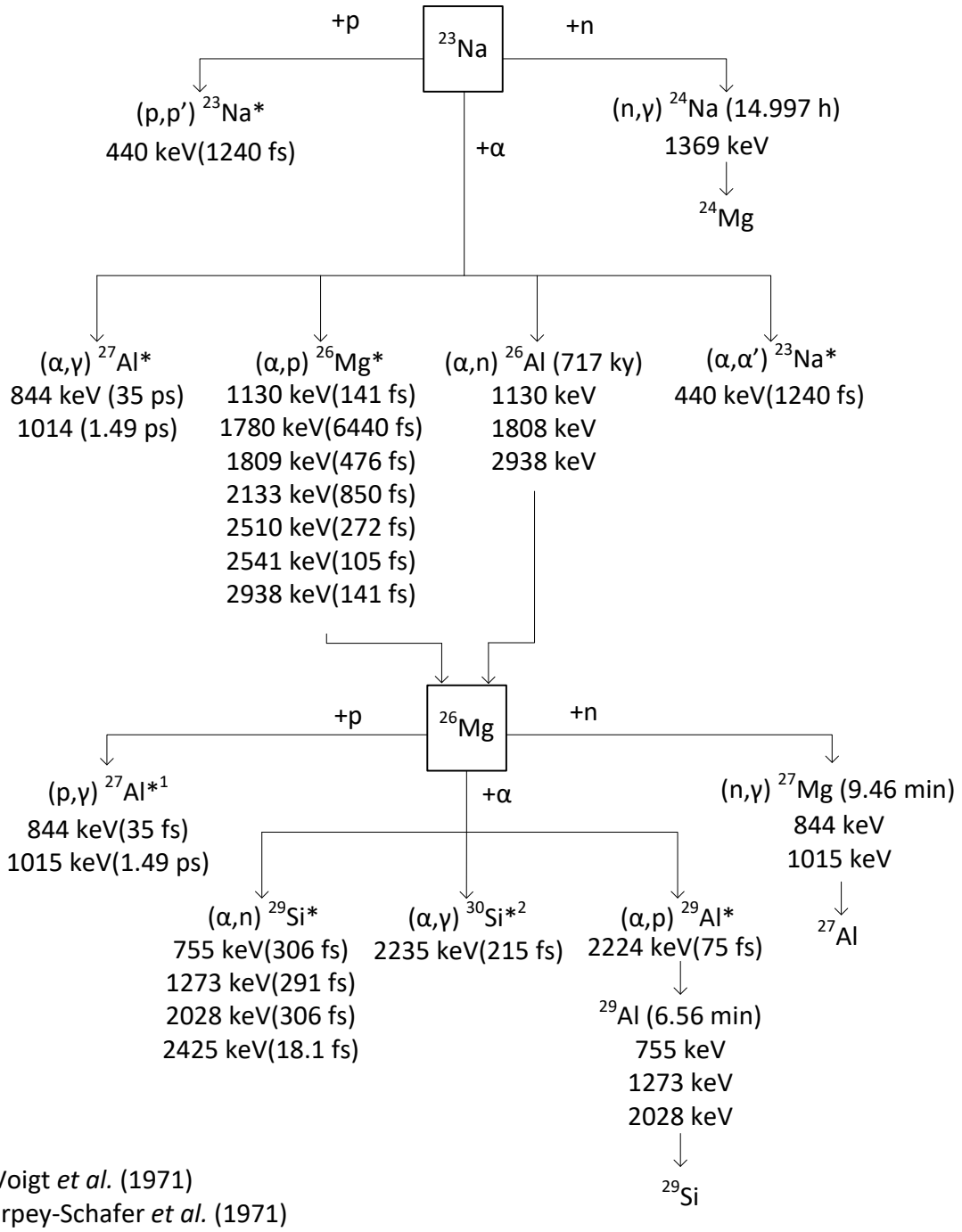

[1] DeVoigt *et al.* (1971)
[2] Sharpey-Schafer *et al.* (1971)

Figure 7 Identified gamma lines from nuclides other than ^{241}Am and its progeny, and suggested reactions based on impurities. The nuclides with an asterisk are emitting gamma rays due to de-excitation. The reference to the gamma lines and corresponding half-lives are taken from the Nudat 2.6 database (2014) unless otherwise stated.

Another kind of impurities are radioactive elements. The spectra of Source 1 and 2 are compared in Figure 8. The figure shows that Source 1 have peaks of ^{239}Np, while these are absent in Source 2. Since the half-life of ^{239}Np is 2.356 days [DDEP, 2018], it is clear that ^{243}Am is present in the source and that the daughter ^{239}Np is in secular equilibrium with ^{243}Am. Therefore, it is possible to calculate an ^{243}Am/^{241}Am-activity ratio. For source 1 and 3 the ratio was $1.444(48)\cdot10^{-6}$ and $2.09(11)\cdot10^{-7}$, respectively.

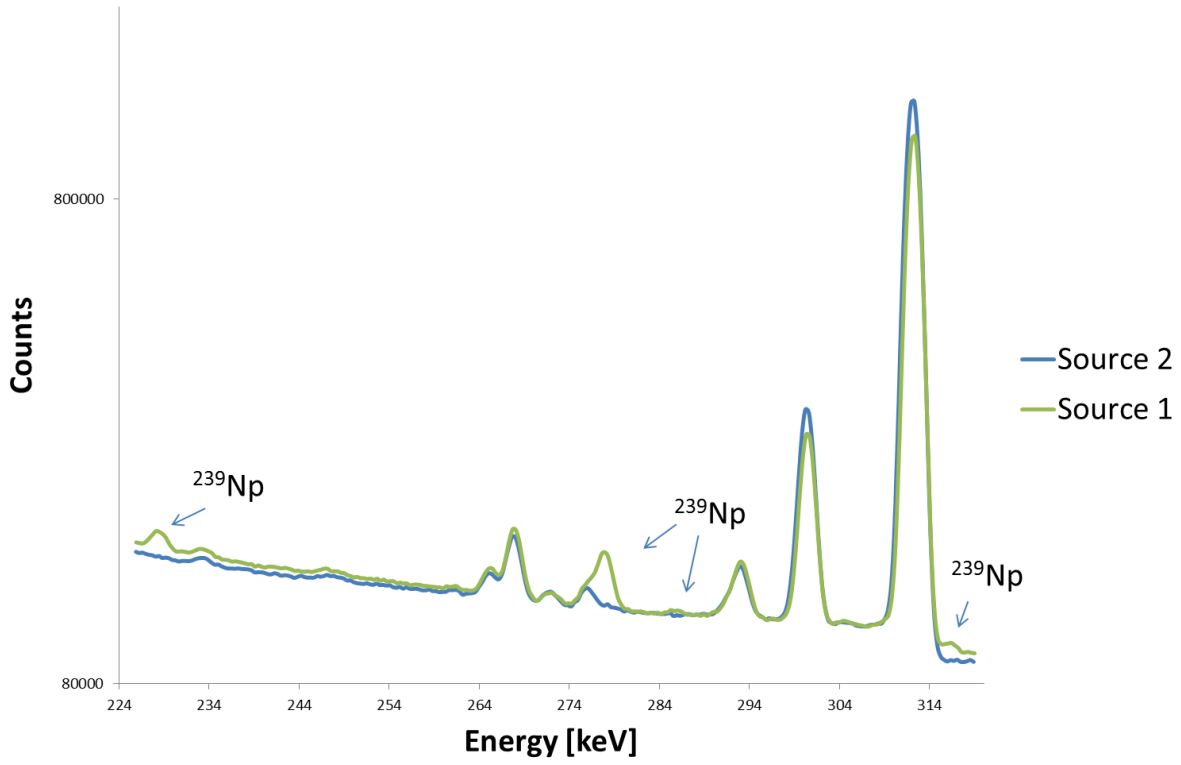

Figure 8 Excerpt of spectra of source 1 and 2.

This study shows that there are a number of potential signatures that can be used to distinguish different ^{241}Am sources. The ^{239}Np content alone was, in this case, enough to distinguish three different sources. Another potentially distinctive signature was the age. The ages of Source 1 and 2 were significantly different. This means that even though these two sources are visually very similar, they can be distinguished with one or two signatures obtained by gamma spectrometric measurements. It may therefore be possible to distinguish sources even though serial numbers are missing. This information could be added in an NNFL containing all indigenous ^{241}Am-sources to be able to investigate found orphan sources in an efficient manner.

5.3 LANTHANIDE PATTERN MEASUREMENTS

5.3.1 Oxide formation measurements

The oxide formation fraction of each of the lanthanides can be seen in Figure 9. The results show that the highest amount of oxides can be found for the lightest of the lanthanides with a decreasing pattern. The lowest oxides are formed for europium and ytterbium. The level of the oxide formation vs element in Figure 9 agrees well with results published by Dulski [1994]. Since the oxide formation is highly dependent on instrumental conditions [Vaughan and Horlick, 1986; Longerich et al, 1987], the variation of the oxide formation may change on a daily basis. However, the relation between oxides remain the same. The fraction of formed hydroxides and hydrides were, if detectable, in the low ppm range. Therefore, the interferences coming from hydroxides and hydrides are considered negligible.

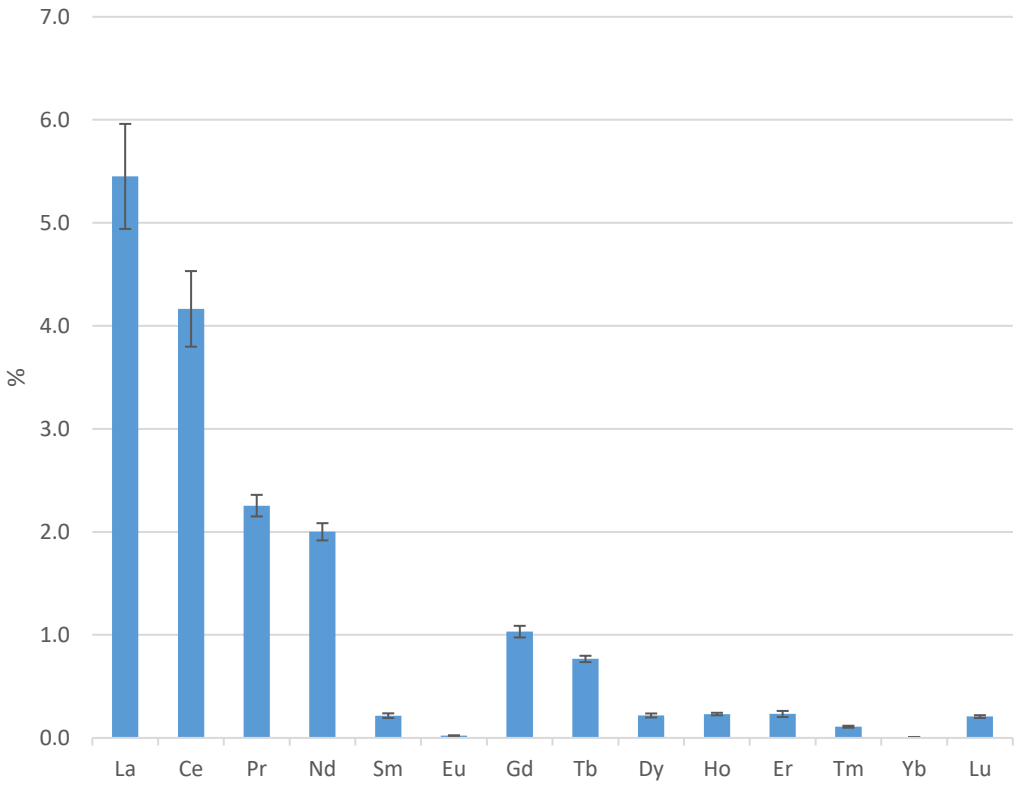

Figure 9 Fraction of oxide formation of the elements in the lanthanide series.

5.3.2 Interfered measurements

The results of the measurements of unseparated samples of REE-2 using the standard sample introduction system can be found in Figure 10. For most elements in the lanthanide series, the results correspond well with the certified values, but for gadolinium and terbium, the measurement results are overestimated. This is due to polyatomic interferences from the light lanthanides, where the oxides of praseodymium and neodymium, $^{141}Pr^{16}O^{+}$ and $^{143}Nd^{16}O^{+}$, end up in the same peak as ^{157}Gd and ^{159}Tb, respectively. The overestimation of these elements were in this case approximately 60% and 40%, respectively.

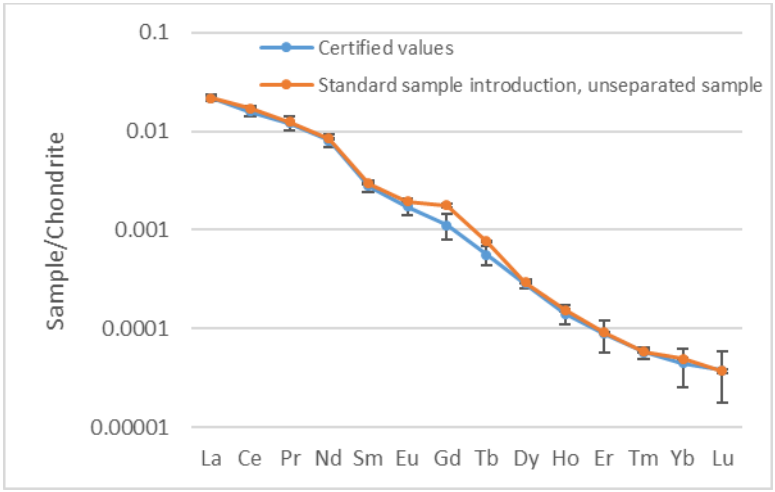

Figure 10 Comparison of the lanthanide pattern for REE-2 between certified values and results from direct measurement using a standard sample introduction system. The uncertainty bars are, in some cases, smaller than the bullets.

5.3.3 Interference-reduced measurements

The resulting lanthanide pattern of REE-2 of the measurements performed with a desolvating sample introduction system and on separated samples, using a standard sample introduction system can be found in Figure 11 and 13, respectively. The results correspond very well with the certified values, i.e. no significant deviations were observed.

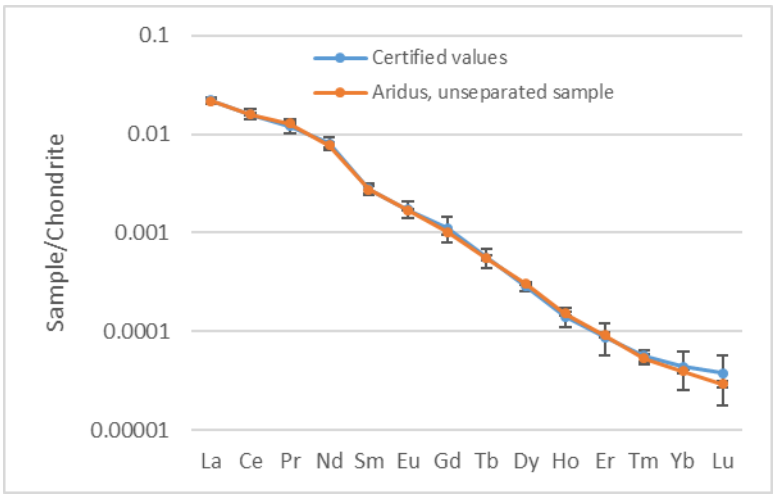

Figure 11 Comparison of the lanthanide pattern for REE-2 between certified values and measured results using a desolvating sample introduction system. The uncertainty bars are, in some cases, smaller than the bullets.

The chemical separation method divides the lanthanides into three fractions. By examining Figure 2, the most effective separation method to remove the most prominent polyatomic interferences would be to separate the lanthanide series into two fractions: La-Eu and Gd-Lu. However, to separate gadolinium from europium in a single separation step using HDEHP has been proven difficult to accomplish [Nash and Jensen, 2000; Morais and Ciminelli, 1998; Morais and Ciminelli, 2007].

A more easily achievable separation method that still solves the issue with interferences from light lanthanides from the heavy ones is to separate the series into three fractions rather than two: La-Nd, Sm-Gd and Tb-Lu. The method development was based on methods previously proposed by Pin and Zalduegui [1997] and Yang et al. [2010]. By increasing the acid concentration, the lanthanides will elute in groups. For the last elution, the acid was changed to nitric acid to avoid the elution of uranium, which will co-elute with the heavy lanthanides when high concentrations of hydrochloric acid is used [Shabana and Ruf, 1977; Kaminski and Nuñez, 2000].

The impact of interferences onto the elements in the lanthanide series after the samples have been separated into three fractions can be seen in Figure 12. The figure shows that, compared to Figure 2 most interferences are removed by the separation. It should be noted that the only element that still does not have any isotope that is free from oxide interferences is lutetium, where ^{175}Lu is interfered by $^{159}Tb^{16}O$. However, this should only be a problem if the amount of terbium is many orders higher than that of lutetium.

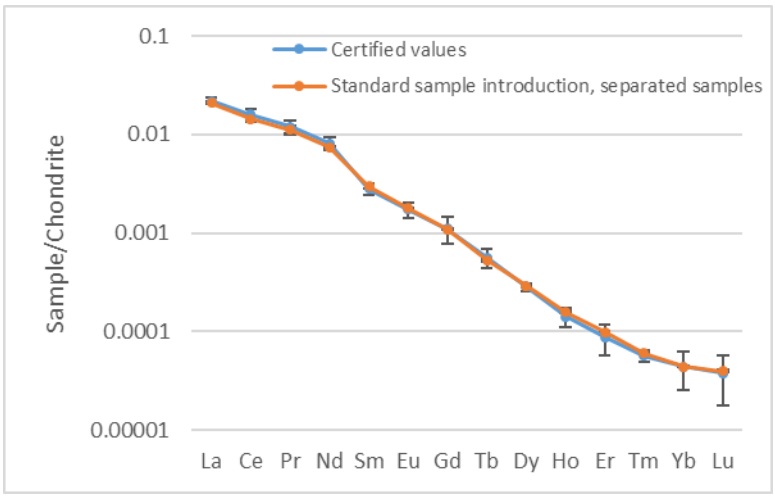

Figure 12 Comparison of the lanthanide pattern for REE-2 between certified values and measured values using a standard sample introduction system after a chemical separation. The uncertainty bars are smaller than the bullets in some cases.

m/z	Ba	La	Ce	Pr	Nd	Sm	Eu	Gd	Tb	Dy	Ho	Er	Tm	Yb	Lu
130	0.11														
131															
132	0.1														
133															
134	2.42														
135	6.59														
136	7.85		0.19												
137	11.23														
138	71.7	0.089	0.25												
139	^{138}BaH	99.911													
140		^{139}LaH	88.45												
141			^{140}CeH	100											
142			11.11	^{141}PrH	27.2										
143			^{142}CeH		12.2										
144					23.8	3.1									
145					8.3										
146	^{130}BaO				17.2										
147	^{130}BaOH				^{146}NdH	15									
148	^{132}BaO				5.8	11.3									
149	^{132}BaOH				^{148}NdH	13.8									
150	^{134}BaO				5.6	7.4									
151	^{135}BaO				^{150}NdH	^{150}SmH	48								
152	^{136}BaO		^{136}CeO			26.7	^{151}EuH	0.2							
153	^{137}BaO					^{152}SmH	52								
154	^{138}BaO		^{138}CeO			22.7	^{153}EuH	2.18							
155	^{138}BaOH	^{139}LaO				^{154}SmH		14.8							
156		^{139}LaOH	^{140}CeO					20.47		0.056					
157			^{140}CeOH	^{141}PrO				15.65							
158			^{142}CeO	^{141}PrOH	^{142}NdO			24.84		0.095					
159			^{142}CeOH		^{143}NdO			^{158}GdH	100						
160					^{144}NdO	^{144}SmO		21.86	^{159}TbH	2.329					
161					^{145}NdO	^{144}SmOH		^{160}GdH		18.889					
162					^{146}NdO					25.475		0.14			
163					^{146}NdOH	^{147}SmO				24.896					
164					^{148}NdO	^{148}SmO				28.26		1.6			
165					^{148}NdOH	^{149}SmO				^{164}DyH	100				
166					^{150}NdO	^{150}SmO					^{165}HoH	33.5			
167					^{150}NdOH	^{150}SmOH	^{151}EuO					22.87			
168						^{152}SmO	^{151}EuOH	^{152}GdO				26.98		0.12	
169						^{152}SmOH	^{153}EuO					^{168}ErH	100		
170						^{154}SmO	^{153}EuOH	^{154}GdO				14.91	^{169}TmH	2.98	
171						^{154}SmOH		^{155}GdO				^{170}ErH		14.09	
172								^{156}GdO		^{156}DyO				21.69	
173								^{157}GdO		^{164}DyOH				16.1	
174								^{158}GdO		^{158}DyO				32.03	
175								^{158}GdOH	^{159}TbO	^{164}DyOH				^{174}YbH	97.4
176								^{160}GdO	^{159}TbOH	^{160}DyO				13	2.6

Figure 13 Isotopes of the lanthanides with abundances [Meija et al, 2016] and their most prominent hydride, oxide and hydroxide interferences in ICP-MS, based on water and nitric acid chemistry. The colour scheme corresponds to separating the lanthanides into three fractions: La-Nd, Sm-Gd and Tb-Lu. The green marked isotopes are not interfered or only slightly interfered and can be used for quantitative determination. The red marked isotopes should be avoided for quantitative measurements. The yellow marked isotopes may be used for determination but are not completely free from interferences. All oxides in the chart refer to ^{16}O.

In the direct measurements, the uranium concentration was approximately 10 µg g^{-1}. This level of heavy matrix did not affect the measurements using the standard sample introduction to any extent. However, the measurements using the desolvating sample introduction suffered from an almost 50% signal suppression due to the high concentration of uranium in the samples. This could however, to some extent, be compensated by the higher sensitivity that can be achieved by the desolvating sample introduction system.

5.3.4 CUP-2

The lanthanide patterns for all three types of measurements, based on the CUP-2 reference material can be seen in Figure 14. The pattern is similar to previously published results [Balboni et al, 2017]. In this case, all three methods provide similar results. This means that for this kind of material, it is possible to use a standard sample introduction system with unseparated samples and still obtain an unaltered lanthanide pattern. However, the amounts of lanthanides in the CUP-2 material are rather low which means that higher concentrations of uranium has to be used in order to have measurable amounts of lanthanides. Since too high concentrations of a heavy matrix such as a uranium matrix causes both signal instability and memory effects, a separation to remove the uranium may be necessary even though the polyatomic interferences are negligible.

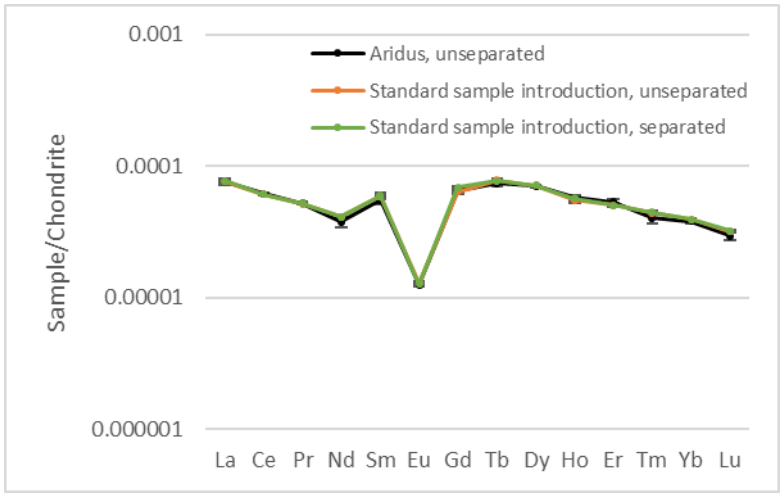

Figure 14 Comparison of the lanthanide pattern for CUP-2 between measurements using all three methods. The uncertainty bars are smaller than the bullets in some cases.

5.3.5 Measurement uncertainties

The lowest measurement uncertainties can be achieved with direct measurement using a standard sample introduction system. Using a desolvating sample introduction system would, in theory, result in just as low uncertainties, but the signal stability is, in general, lower for this kind of sample introduction, which increases the measurement uncertainty slightly. The highest uncertainty was found for the separated samples. This is due to the uncertainties in the yield determination. Even though a standard sample introduction system is used, the combined uncertainty is significantly higher. The measurement uncertainties for the separated samples were on average around 3% with a few exceptions where the combined uncertainty was higher.

5.4 EXTERNAL CALIBRATION FOR TRACE ELEMENT ANALYSIS

5.4.1 OLS vs WLS

The effect of an OLS compared to a WLS regression can be seen in Figure 15. On closer inspection, the calibration function based on OLS regression is strongly overestimating the intercept of the line. This, together with high uncertainty of the intercept, will cause the detection limit to be very high in the case of OLS. The WLS regression, on the other hand, provides a calibration function that corresponds well at concentrations close to zero. The OLS detection limit in the case of Figure 15 was 10 pg g^{-1} while the corresponding detection limit for WLS was 14 fg g^{-1}.

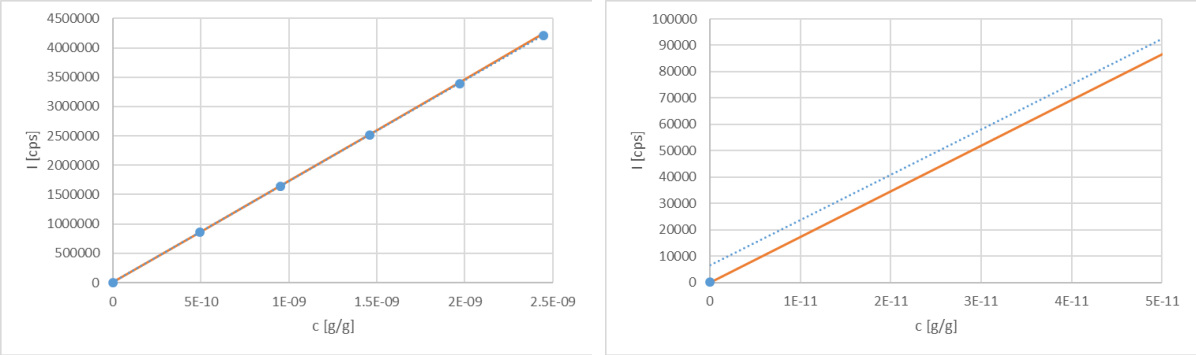

Figure 15 Left: Calibration lines based on calibration data on holmium. The blue dots are the data points used for the calibration, the dotted line is the OLS based on these data points. The orange line is the corresponding WLS regression. Right: The same calibration lines in the low concentration part of the calibration.

5.4.2 Quality control samples

The results of the measurement of the 1 ng g^{-1} QC samples and the comparison to the certified value using WLS regression can be seen in Figure 16. The figure shows that the concentration of some of the elements in Standard solution 1 deviates from the certified values. If the zeta score is larger than 2, the difference between measured and certified value is not covered by their uncertainties on an approximate 95% confidence level. The measurement results of Standard solution 2, on the other hand, agreed well with the certified values. One possibility is that the difference between the CRM is a result of differing isotopic compositions in the solutions. Therefore, all masses between 137 and 176 in one sample from each CRM was measured and compared. There were no significant differences in isotopic compositions between the materials. These results could imply that, for some elements, there is a difference in concentration between Standard solution 1 and the CRM used for calibration not covered by the uncertainty of the two solutions. Therefore, this discrepancy needs to be addressed.

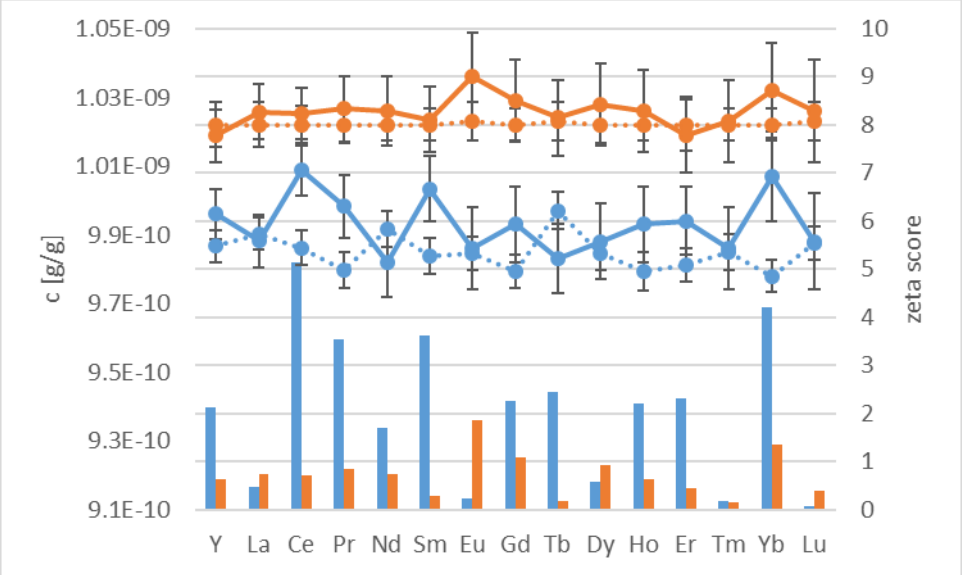

Figure 16 Measurement results and certified values of each element together with the calculated zeta score. The blue series correspond to Standard solution 1 and the orange series corresponds to Standard solution 2. The continuous lines are the measured values and the dashed lines are certified values. The bars corresponds to the calculated zeta scores.

According to ISO Guide 33:2015, any discovered bias should primarily be reduced or eliminated, secondly corrected for and the additional uncertainty added to the uncertainty budget and thirdly, if these approaches are regarded as impossible to carry through, the bias should be included in the uncertainty budget [ISO 33:2015]. Since it is difficult to determine which of the solutions that has the correct concentration, the third approach, to include the bias in the uncertainty budget was chosen. Therefore, an extra input quantity, δ, was added to the model equation for the calculation of the concentration of isotope *j* in sample *i*, $c_{i,j}$, of the measured sample where m_j is the intercept and k_j is the slope of the calibration function and $I_{corr,i,j}$ is the intensity of isotope *j* in the sample *i* corrected for dead-time and internal standard:

$$c_{i,j} = \frac{I_{corr,i,j} - m_j}{k_j} + \delta \tag{25}$$

δ has value 0 and the uncertainty of δ, $u(\delta)$, was increased until the zeta score was 2. This approach ensures that the result of the measurement of the QC sample corresponds to the certified value within uncertainties at the 95% confidence level and has previously been applied on replicate samples by Kessel et al. [2008] in a similar fashion. This δ and its uncertainty would, in other cases, be added to

samples that are measured in the same measurement sequence. It should be noted that if the choice was made to use the same CRM for the calibration as for the QC sample, this inconsistency would not have been detected and the risk of reporting analytical results containing bias or underestimated uncertainties would be considerable.

The initial uncertainties of the measurements varied between 0.7 and 1.5% depending on element. After some of the measurands had received an extra uncertainty the measurement uncertainty increased to about maximum 3%, see Figure 17. The, in most cases, low combined uncertainty is largely a result from performing the sample preparation gravimetrically. The results from volumetric sample preparation gives uncertainties around 3%. Most of the uncertainty in this case can be explained by the addition of internal standard and the uncertainty in the estimation of the slope. The uncertainty of the pipettes were evaluated according to ISO 8655-6 [2002]. For volumes less than 1 ml the combined uncertainty was evaluated to 0.8%, k=1 and 0.4% for volumes larger than 5 ml. Due to the relatively high measurement uncertainty, there was no need for the extra uncertainty, u(δ), for any element, at the 1 ng g^{-1} level for the volumetric samples.

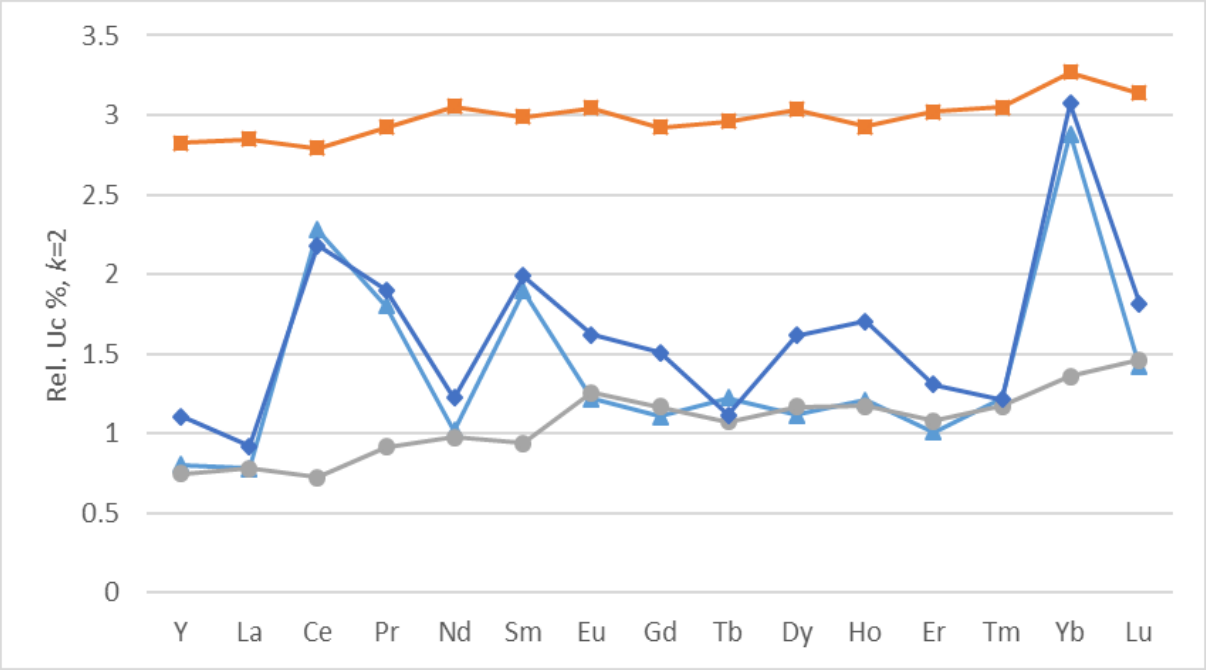

Figure 17 Relative uncertainties for the measured 1 ng g^{-1} control samples when an extra uncertainty has been added when necessary. The following data are evaluated using weighted linear regression: The triangles correspond to Standard solution 1, the circles to Standard solution 2 both with dilutions performed gravimetrically, the squares to Standard solution 1 in the case where dilutions were performed volumetrically. The diamonds correspond to the control sample from Standard solution 1 evaluated using OLS.

It can be noted that the measurement uncertainty of Standard solution 1 using either OLS or WLS results in practically the same uncertainties at the 1 ng g^{-1} level. This implicates that the OLS regression works rather well in this part of the calibration. At the 100 pg g^{-1} level, however, the measurement uncertainty is substantially higher for the results based on OLS, see Figure 18. This is mainly due to the large uncertainty in the intercept that follows from using OLS regression on heteroscedastic data [Ketkar and Bzik, 2000].

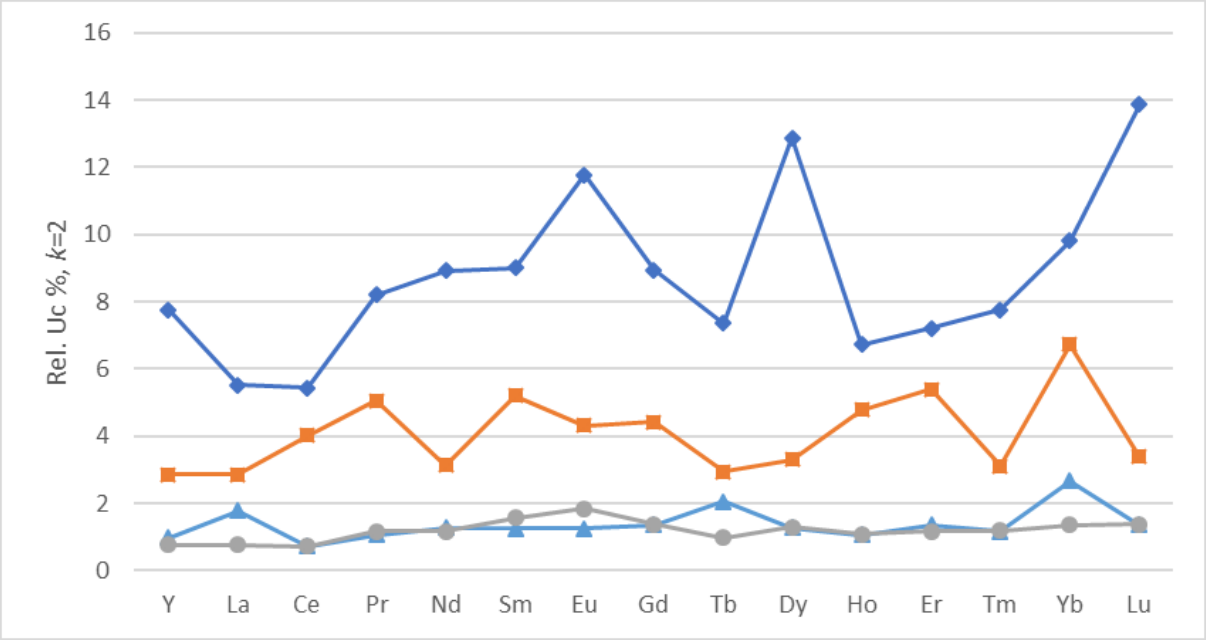

Figure 18 Relative uncertainties for the measured 100 pg g^{-1} control samples when an extra uncertainty has been added when necessary. The following data are evaluated using WLS: The triangles correspond to Standard solution 1, the circles to Standard solution 2 both with dilutions performed gravimetrically and the squares to Standard solution 1 in the case where dilutions were performed volumetrically. The diamonds correspond to the control sample from Standard solution 1 evaluated using OLS.

6 CONCLUSIONS

This work has shown the development of a series of signatures that are useful in the field of nuclear forensics. The work also highlights some problems that may be encountered in measurements of nuclear forensic signatures. One of the primary goals in nuclear forensics is to achieve accurate and precise measurements. There should be no ambiguity in the obtained analysis results. Therefore, the method development in nuclear forensics strive to reduce measurement uncertainty and to understand measurement processes to the extent that the measurement uncertainties are fully understood and accounted for.

Paper I highlights the difficulty of categorizing uranium automatically using low-resolution instruments. Even though a categorization carried out with such an instrument hardly would be the only measurement performed in a nuclear forensic investigation, the direction of the initial investigation may rely upon that measurement. The progress of the investigation could be impeded if the categorization would be incorrect. Therefore, it is important to be aware of the limitations of low-resolution measurements.

Paper II illustrates a number of possible signatures that can be used to identify ^{241}Am sources in cases where labels and serial numbers are destroyed or unreachable. Corresponding signatures should be possible to use in other types of sources with an alpha emitting nuclide. These signatures would be useful to populate an NNFL, since the combination of multiple signatures could single out or at least narrow down the identity of a source found out of regulatory control.

The work in **Paper III** investigated the prospect of maximizing accuracy and precision in measurements of lanthanides for geolocation of uranium using ICP-MS. Polyatomic interferences in measurements of the lanthanide series are well-known but have been neglected since the conclusion of geological origin is based on visual inspection of the chondrite normalized lanthanide pattern. If closer examinations need to be made, as often in the case of nuclear forensics, the interferences may start to affect conclusions drawn from the lanthanide measurement results. Since the oxide formation may vary on a daily basis, the impact of interfering species may also vary. This means that if two identical materials are measured on different occasions, the lanthanide measurements could indicate that the materials have different provenance. Therefore, by correcting for or avoiding the polyatomic interferences, the possibility to use the lanthanide series for comparison between materials in different parts of the nuclear fuel production, opens up.

Paper IV highlights the intricacy of measuring trace elements using external calibration and mass spectrometry. Since trace elements can be expected to be very low in concentration in uranium materials, the importance of providing an accurate calibration over the whole calibration range cannot be emphasized enough. The study shows that, in order to perform measurements with high confidence, a number of parameters need to be considered. The choices that are made considering type of regression and how the sample preparation has been performed, are crucial for the quality of the measurement results and at the end on the decision making process where the measurement result is an important part.

7 ACKNOWLEDGEMENTS

Along the way, I have had a lot of people to help me. Therefore, I would like to thank:

- My supervisor Henrik for the never-ending stream of ideas and passion for science. I am grateful for all the discussions we have had over the years.

- My supervisor Christian for providing feedback on my papers and guiding me through Chalmers' administration.

- Angelica and Stina, my partners in crime, my colleagues and good friends. I owe you a lot.

- My colleagues Annika, Sofia and Petra, you are all role models for female scientists. Thank you for your support.

- Micce for the help with the measurements of the ^{241}Am-sources and all the bad puns you deliver whether we like it or not.

- My remaining colleagues at the Department for Radioactive substances. Thank you for all the laughs around the coffee table, AW's and past and future hallway parties.

- Leif Persson for valuable discussions about what I thought was basic maths.

- The rest of my colleagues at FOI, CBRN Defence and Security. It is amazing how much expertise that can fit in a house in the middle of a forest.

- The Swedish Defence Research Agency for giving me the opportunity to complete my thesis.

- My fellow colleagues in the nuclear forensics community, participating in the ITWG meetings. Meeting you once in a while is a great inspiration.

- Einar for your contagious optimism and for proofreading the thesis with reluctant joy.

- My family for believing in me even though you might not always know what I work with.

- The Swedish Civil Contingencies Agency, the Swedish Radiation Safety Authority and the Ministry of Defence for funding my research.

8 ABBREVIATIONS

ANSI	American National Standards Institute
CRM	Certified Reference Material
DU	Depleted uranium
ESA	Electrostatic Analyzer
FTIR	Fourier Transform Infrared Spectrometry
GC-MS	Gas Chromatography Mass Spectrometry
GICNT	Global Initiative to Combat Nuclear Terrorism
HDEHP	Di-(2-ethylhexyl)-phosphoric acid
HEU	Highly enriched uranium
HPGe	High Purity Germanium detector
IAEA	International Atomic Energy Agency
ICP-MS	Inductively Coupled Plasma - Mass Spectrometry
ISO	International Organization for Standardization
ITDB	Incident and Trafficking Data Base
ITWG	Nuclear Forensics International Technical Working Group
LEU	Low enriched uranium
LREE	Light rare earth elements
MCNPX	Monte Carlo N-Particle eXtended
NAA	Neutron activation analysis
NNFL	National Nuclear Forensics Library
NPT	Treaty on the Non-proliferation of Nuclear Weapons
NU	Natural uranium
OLS	Ordinary least squares regression
RDD	Radiological Dispersion Device
SEM	Scanning Electron Microscope
SIMS	Secondary Ion Mass Spectrometry
SME	Subject Matter Expert
SSAMS	Single Stage Accelerator Mass Spectrometry
TEM	Transmission Electron Microscopy
TIMS	Thermal Ionisation Mass Spectrometry
UOC	Uranium ore concentrate
VGSL	Virtual Gamma Spectroscopy Laboratory
WLS	Weighted least squares regression
XRD	X-ray Diffraction
XRF	X-ray Fluorescence

9 REFERENCES

Almeida A.M., Castel-Branco M.M., Falcão A.C., Linear regression for calibration lines revisited: weighting schemes for bioanalytical methods, Journal of Chromatography B, 774 (2002) 215-222.

Alstad J., Augustson J. H., Danielssen T., Farbu L., A comparative study of the rare earth elements in extraction by HDEHP/Shell Sol T from nitric and sulfuric acid solutions, International Solvent Extraction Conference (1974) 1083-1102.

American National Standard Performance Criteria for Hand-Held Instruments for the Detection and Identification of Radionuclides, ANSI N42.34-2006 (Revision of ANSI N42.34-2003), c1-35, 2007.

Anders E., Grevesse N., Abundances of the elements: Meteoritic and solar, Geochim. Cosmochim. Acta, 53 (1989) 197-214.

Appelblad P., Baxter D., A model for calculating dead-time and mass discrimination correction factors from inductively coupled plasma mass spectrometry calibration curves, J. Anal. At. Spectrom., 15 (2000) 557-560.

Arnold L., The history of nuclear weapons: The Frisch-Peierls memorandum on the possible construction of atomic bombs of February 1940, Cold War History, 3:3 (2003) 111-126.

Balboni E., Simonetti A., Spano T., Cook N., Burns P., Rare-earth element fractionation in uranium ore and its U(VI) alteration minerals, Applied Geochemistry, 87 (2017) 84-92.

Beauchemin D., McLaren J. W., Berman S. S., Study of the effects of concomitant elements in inductively coupled plasma mass spectrometry, Spectrochim. Acta, 3 (1987) 467-490.

Becker J. S., Inorganic Mass Spectrometry, Principles and Applications, John Wiley & Sons Ltd, Chichester, West Sussex, England, 2007.

Blackadar J.M., Bounds J.A., Hypes P.A., Mercer D.J., Sullivan C.J., Evaluation of Handheld Isotope Identifiers, LA-UR-03-2742, Los Alamos National Lab., Los Alamos, NM, 2003.

Borgardt J., Canaday J., Chamberlain D., Results from the second Galaxy Serpent web-based tabletop exercise utilizing the concept of nuclear forensics libraries, J. Radioanal. Nucl. Chem., 311 (2017) 1517-1524.

Boulyga S. F., Cunningham J. A., Macsik Z., Hiess J., Peńkin M. V., Walsh S. J., Development, validation and verification of an ICP-MS procedure for a multi-element analysis of uranium ore concentrates, J. Anal. At. Spectrom., 32 (2017) 2226-2237.

Bulska E., Danko B., Dybczyński R. S., Krata A., Kulisa K., Samczyński Z., Wojciechowski M., Inductively coupled plasma mass spectrometry in comparison with neutron activation and ion chromatography with UV/VIS detection for the determination of lanthanides in plant materials, Talanta, 97 (2012) 303-311.

Catz A.L., Amiel S., Study of lifetimes of nuclear levels by Doppler broadening attenuation using a Ge(Li) gamma-ray spectrometer, Nucl. Phys. A, 92 (1967) 222-232.

Cheong C., Kim N., Yi K., Jo H.J., Jeong Y-J., Kim Y., Koh S.M., Iizuka T., Recurrent rare earth element mineralization in the northwestern Okcheon Metamorphic Belt, Korea: SHRIMP U-Th-Pb

geochronology, Nd isotope geochemistry, and tectonic implications, Ore Geology Reviews, 71 (2015) 99-115.

Code of Conduct on the Safety and Security of Radioactive Sources, IAEA/CODEOC/2004, Vienna, Austria, 2004.

Dampare S. B., Asiedu D. K., Osae S., Nyarko B. J. B., Banoeng-Yakubo B., Determination of rare earth elements by neutron activation analysis in altered ultramafic rocks from the Akwatia District of the Birim diamondiferous field, Ghana, J. Radioanal. Nucl. Chem., 265 (2005) 101-106.

Decay Data Evaluation Project (DDEP), http://www.nucleide.org/DDEP_WG/DDEPdata.htm, accessed in January 2018.

Deming W. E. Statistical Adjustment of Data, Dover, New York, 1964.

Development of a National Nuclear Forensic Library: A System for the Identification of Nuclear or Other Radioactive Material out of Regulatory Control, IAEA-TDL-009, IAEA, Vienna, 2018.

De Voigt M.J.A., Maas J.W., Veenhof D., Van Der Leun C., The reaction $^{23}Na(\alpha,\gamma)^{27}Al$ (I). Yield curve, excitation energies and branchings of ^{27}Al levels, Nucl. Phys., A170 (1971) 449-466.

Dulski P., Interferences of oxide, hydroxide and chloride analyte species in the determination of rare earth elements in geological samples by inductively coupled plasma-mass spectrometry, Fresenius J. Anal. Chem., 350 (1994) 194-203.

Eppich G. R., Williams R. W., Gaffney A. M., Schorzman K. C., ^{235}U-^{231}Pa age dating of uranium materials for nuclear forensic investigations, J. Anal. At. Spectrom., 28 (2013) 666-674.

Estep R.J., Rawool-Sullivan M., Miko D., A method for correcting NaI spectra for attenuation losses in hand-held instrument applications. IEEE Transactions on Nuclear Science, 45 (1998) 1022-1028.

Evans E. H., Giglio J. J., Interferences in Inductively Coupled Plasma Mass Spectrometry – A Review, J. Anal. At. Spectrom., 8 (1993) 1-18.

Fisher D., History of the International Atomic Energy Agency, The First Forty Years, IAEA, Austria, 1997.

Frimmel H. E., Schedel S., Brätz H., Uraninite chemistry as forensic tool for provenance analysis, Appl. Geochem., 48 (2014) 104-121.

Fryer B. J., Taylor R. P., Rare-earth element distributions in uraninites: Implications for ore genesis, Chem. Geology, 63 (1987) 101-108.

Funderberg R., Arevalo Jr R., Locmelis M., Adachi T., Improved Precision and Accuracy of Quantification of Rare Earth Element Abundances via Medium-Resolution LA-ICP-MS, J. Am. Soc. Mass. Spectrom., 28 (2017) 2344-2351.

Gehrke R.J, East L.V., Information in spectra from sources containing “aged” ^{241}Am as from TRU waste, Waste Management, 20 (2000) 555–559.

Gehrke R.J., Baker J.D., Hartwell J.K., Riddle C.L., McGrath C.A., Measurement of neutron-to-γ-ray production ratios from (α,n) reactions for their application to assay TRU waste, Nucl. Instr. Meth. Phys. Res. A, 511 (2003) 444-456.

GICNT, 2018, http://www.gicnt.org/, retrieved January 2018.

Gilmore, G.R., Practical Gamma-ray Spectrometry, 2nd Edition, John Wiley & Sons Ltd, Chippenham, United Kingdom, 2011.

Groopman E., Grabowski K., Fahey A., Kööp L., Rapid, molecule-free, in situ rare earth element abundances by SIMS-SSAMS, J. Anal. At. Spectrom.,, 32 (2017) 2153-2163.

Hahn O., Strassmann F., Nachweis der Entstehung aktiver Bariumisotope aus Uran und Thorium durch Neutronenbestrahlung; Nachweis weiterer aktiver Bruchstücke bei der Uranspaltung, Naturwiss., 37 (1939) 89-95.

Harris D. C., Quantitative Chemical Analysis, 6th edition, W. H. Freeman and Company, New York, United States, 2003.

Healey G., Button P., Change in impurities observed during the refining and conversion processes, Esarda Bulletin, 49 (2013) 57-65.

Holmgren Rondahl S., Pointurier F., Ahlinder L., Ramebäck H., Marie O., Ravat B., Delaunay F., Young E., Blagojevic N., Hester J. R., Thorogood G., Nelwamondo A. N., Ntsoane T. P., Roberts S. K., Holliday K. S., Comparing results of X-ray diffraction, μ-Raman spectroscopy and neutron diffraction when identifying chemical phases in seized nuclear material, during a comparative nuclear forensics exercise, 315 (2018) 395-408.

Hofstetter K., Beals D., Odell D., Uranium detection using small scintillators in a maritime environment. J. Radioanal. Nucl. Chem., 276 (2008) 433-439.

Hubaux A., Vos G., Decision and Detection Limits for Linear Calibration Curves, Analytical Chemistry, 42 (1970) 849-855.

Hutcheon I.D., Kristo M.J., Knight K.B., Non-proliferation Nuclear Forensics, Uranium – Cradle to Grave, Min. Assoc. of Canada, pp. 377-394, 2013.

IAEA Safeguards Glossary, 2001 Edition, International Nuclear Verification Series No. 3, Vienna, Austria, 2002.

Incident and Trafficking Database (ITDB), http://www-ns.iaea.org/security/itdb.asp, retrieved January 2019.

ISO Guide 33:2015 (2015) Reference materials – Good practice in using reference materials, the International Organization for Standardization, Geneva, Switzerland.

ISO/IEC Guide 98-3:2008 (2008) Uncertainty of measurement – Part 3: Guide to the expression of uncertainty in measurement, the International Organization for Standardization, Geneva, Switzerland.

ISO 8655-6:2002 (2002) Piston-operated volumetric apparatus – Part 6: Gravimetric methods for the determination of measurement error, the International Organization for Standardization, Geneva, Switzerland.

ISO 13528:2015 (2015) Statistical methods for use in proficiency testing by interlaboratory comparison, the International Organization for Standardization, Geneva, Switzerland.

Jakubowski N., Moens L., Vanhaecke F., Sector field mass spectrometers in ICP-MS, Spectrochim. Acta, 53B (1998) 1739-1763.

Jakubowski N., Prohaska T., Rottmann L., Vanhaecke F., Inductively coupled plasma- and glow discharge plasma-sector field mass spectrometry, 26 (2011) 693-726.

Kaminski M., Nuñez L., Separation of Uranium from Nitric- and Hydrochloric-Acid Solutions with Extractant-Coated Magnetic Microparticles, Separation Science and Technology, 35:13 (2000) 2003-2018.

Keegan E., Kristo M. J., Colella M., Robel M., Williams R., Lindwall R., Eppich G., Roberts S., Borg L., Gaffney A., Plaue J., Wong H., Davis J., Loi E., Reinhard M., Hutcheon I., Nuclear forensic analysis of an unknown uranium ore concentrate sample seized in a criminal investigation in Australia, Forensic Science International, 240 (2014) 111-121.

Kessel R., Berglund M., Wellum R., Application of consistency checking to evaluation of uncertainty in multiple replicate measurements, Accred Qual Assur, 13 (2008) 293-298.

Ketkar S. N., Bzik T. J., Calibration of Analytical Instruments. Impact of Nonconstant Variance in Calibration Data, Anal. Chem., 72 (2000) 4762-4765.

Knoll G.F., Radiation Detection and Measurement, John Wiley & Sons, New York, United States, 2000.

Kristo M. J., Keegan E., Colella M., Williams R., Lindvall R., Eppich G., Roberts S., Borg L., Gaffney A., Plaue J., Knight K., Loi E., Hotchkis M., Moody K., Singleton M., Robel M., Hutcheon I., Nuclear forensic analysis of uranium oxide powders interdicted in Victoria, Australia, Radiochim. Acta, 103 (2015) 487-500.

Kristo M.J., Tumey S.J., The state of nuclear forensics, Nucl. Inst. Meth. Phys. B, 294 (2013) 656-661.

Leggitt J., Inn K., Goldberg S., Essex R., LaMont S., Chase S., Nuclear forensics – metrological basis for legal defensibility, J. Radioanal. Nucl. Chem., 282 (2009) 997-1001.

Litwak R. S., Deterring Nuclear Terrorism, Wilson Center, Washington DC, United States, 2016, ISBN 978-1-938027-59-8.

Lobato L.M., Pimentel M.M., Cruz S.C.P., Machado N., Noce C.M., Alkmim F.F., U-Pb geochronology of the Lagoa Real uranium district, Brazil: implications for the age of the uranium mineralization, J. South Am. Earth Sci., 58 (2015) 129-140.

Longerich H., Fryer B., Strong D., Kantipuly C., Effects of operating conditions on the determination of the rare earth elements by inductively coupled plasma-mass spectrometry (ICP-MS), Spectrochimica Acta,, 42B (1987) 75-92.

Lützenkirchen K., Wallenius M., Varga Z., Wiss T., Knott A., Nicholl A., Mayer K., Nuclear forensics on uranium fuel pellets, Radiochim. Acta, 107 (2019) 635-643.

Mayer K., Glaser A., Nuclear Forensics, From: Routledge Handbook of Nuclear Proliferation and Policy, Routledge, ISBN 978-1-1360-1248-8, London, United Kingdom, 2015.

Meija J., Coplen T. B., Berglund M., Brand W. A., De Bièvre P., Gröning M., Holden N. E., Irrgeher J., Loss R. D., Walczyk T., Prohaska T., Isotopic compositions of the elements 2013 (IUPAC Technical Report) Pure Appl. Chem., 88(3) (2016) 293-306.

Meitner L., Frisch O.R., Disintegration of Uranium by Neutrons: a New Type of Nuclear Reaction, Nature, 143 (1939) 239-240.

Mercadier J., Cuney M., Lach P., Boiron M-C., Bonhoure J., Richard A., Leisen M., Kister P., Origin of uranium deposits revealed by their rare earth element signature, Terra Nova, 23 (2011) 264-269.

Miller J. N., Miller J. C., Statistics and Chemometrics for Analytical Chemistry, 6 ed, Pearson Education Limited, ISBN 978-0-273-73042-2, Harlow, Essex, England, 2010.

Morais C. A., Ciminelli V. S. T., Recovery of europium from a rare earth chloride solution, Hydrometallurgy, 49 (1998) 167-177.

Morais C. A., Ciminelli V. S. T., Selection of solvent extraction reagent for the separation of europium(III) and gadolinium(III), Minerals Engineering, 20 (2007) 747-752.

Nash K. L., Jensen M. P., Analytical Separations of the Lanthanides: Basic Chemistry and Methods, Chapter 180 in Handbook on the Physics and Chemistry of Rare Earths, Vol. 28, Elsevier Science B.V., North-Holland, 2000.

Nelms S. M., ICP Mass Spectrometry Handbook, Blackwell Publishing Ltd, ISBN 978-1-4051-0916-1, Oxford, UK, 2005.

Nelson K. E., Gosnell T. B., Knapp D. A., The effect of energy resolution on the extraction of information content from gamma-ray spectra. Nucl. Inst. Meth. Phys. A, 659 (2011) 207-214.

Nelwamondo A. N., Colletti L. P., Lindvall R. E., Vesterlund A., Xu N., Hiong Jun Tan A., Eppich G. R., Genetti V. D., Kokwane B. L., Lagerkvist P., Pong B. K., Ramebäck H., Tandon L., Rasmussen G., Varga Z., Wallenius M., Uranium assay and trace element analysis of the fourth collaborative material exercise samples by the modified Davies-Gray method and the ICP-MS/OES techniques, J Radioanal Nucl Chem, 315 (2018) 379-394.

Nguyen C.T., Zsigrai J., Basic characterization of highly enriched uranium by gamma spectrometry. Nucl. Inst. Meth. Phys. B, 246 (2006) 417-424.

NPT/CONF.2015/13, Activities of the International Atomic Energy Agency relevant to article III of the Treaty on the Non-Proliferation of Nuclear Weapons: background paper prepared by the secretariat of the International Atomic Energy Agency, Review Conference of the Parties to the Treaty on the Non-Proliferation of Nuclear Weapons, Conference paper, 2015.

Nuclear Forensics Support, IAEA Nuclear Security Series No.2: Technical Guidance, Vienna, 2006.

Nuclear Forensics in Support of Investigations: Implementing Guide, IAEA Nuclear Security Series No.2-G (rev.1), Vienna, 2015.

Nuclear Security Recommendations on Nuclear and Other Radioactive Material out of Regulatory Control, IAEA Nuclear Security Series No.15, Vienna, 2011.

NuDat 2.6 database, 2014, http://www.nndc.bnl.gov/nudat2/, National Nuclear Data Center, Brookhaven National Laboratory, USA.

Nygren U., Ramebäck H., Nilsson C., Age determination of plutonium using inductively coupled plasma mass spectrometry, J. Radioanal. Nucl. Chem., 272 (2007) 45-51.

Peppard D. F., Mason G. W., Maier J. L., Driscoll W. J., Fractional extraction of the lanthanides as their di-alkyl orthophosphates, J. Inorg. Nucl. Chem., 4 (1957) 334-343.

Pibida L., Unterweger M., Karam L.R., Evaluation of Handheld Radionuclide Identifiers. Journal of Research of the National Institute of Standards and Technology, 109 (2004) 451-456.

Pin C., Zalduegui J. F. S., Sequential separation of light rare-earth elements, thorium and uranium by miniaturized extraction chromatography: Application to isotopic analyses of silicate rocks, Anal. Chim. Acta, 339 (1997) 79-89.

Plenteda R., A Monte Carlo Based Virtual Gamma Spectrometry Laboratory. Atominstitut der Österreichischen Universitaten, 2002.

Prohaska T., Hann S., Latkoczy C., Stingeder G., Determination of rare earth elements U and Th in environmental samples by inductively coupled plasma double focusing sector field mass spectrometry (ICP-SMS), J. Anal. At. Spectrom., 14 (1999) 1-8.

Qureshi I. H., McClendon L. T., LaFleur P. D., Radiochim. Acta, 12 (1969) 107-111.

Ramebäck H., Nygren U., Lagerkvist P., Verbruggen A., Wellum R., Skarnemark G., Basic characterization of ^{233}U: Determination of age and ^{232}U content using sector field ICP-MS, gamma spectrometry and alpha spectrometry, Nucl. Inst. Meth Phys. B, 266 (2008) 807-812.

Ramebäck H., Nygren U., Tovedal A., Ekberg C., Skarnemark G., Uncertainty assessment in gamma spectrometric measurements of plutonium isotope ratios and age, Nucl. Instr. Meth. Phys. Res. B, 287 (2012) 56–59.

Ramebäck H., Lindgren P., Uncertainty evaluation in gamma spectrometric measurements: Uncertainty propagation versus Monte Carlo simulation, Appl. Rad. Isot., 142 (2018) 71-76.

Raposo F., Evaluation of analytical calibration based on least-squares linear regression for instrumental techniques: A tutorial review, Trends in Analytical Chemistry, 77 (2016) 167-185.

Raut N. M., Huang L-S., Aggarwal S. K., Lin K-C., Determination of lanthanides in rock samples by inductively coupled plasma mass spectrometry using thorium as oxide and hydroxide correction standard, Spectrochim. Acta, 58B (2003) 809-822.

Reed T. C., Stillman D. B., The Nuclear Express: A political history of the bomb and its proliferation, Zenith Press, Minneapolis, USA, 2009.

Rydberg J., Musikas C., Choppin G. R., Principles and Practices of Solvent Extraction, Marcel Dekker, New York, 1992.

Sayago A., Asuero A., Fitting Straight Lines with Replicated Observations by Linear Regression: Part II. Testing for Homogeneities of Variances, Critical Reviews in Analytical Chemistry, 34 (2004) 133-146.

Shabana R., Ruf H., Extraction and separation of uranium, thorium and cerium from different mixed media with HDEHP, J Radioanal Chem,, 36 (1977) 389-397.

Sharpey-Schafer J.F., Alderson P.R., Bailey D.C., Durell J.L., Greene M.W., James A.N., Lifetimes and decays of energy levels in ^{30}Si and ^{30}P, Nucl. Phys., A167 (1971) 602-624.

Simitchiev K., Stefanova V., Kmetov V., Andreev G., Sanchez A., Canals A., Investigation of ICP-MS spectral interferences in the determination of Rh, Pd, and Pt in road dust: Assessment of correction algorithms via uncertainty budget analysis and interference alleviation by preliminary acid leaching, Talanta, 77 (2008) 889-896.

Spano T. L., Simonetti A., Balboni E., Dorais C., Burns P. C., Trace element and U isotope analysis of uraninite and ore concentrate: Applications for nuclear forensic investigations, Appl. Geochem., 84 (2017) 277-285.

Sprinkle Jr J. K., Christiansen A., Cole R., Collins M. L., Hsue S. T., Knepper P. L., McKown T. O., Siebelist R., Low-resolution gamma-ray measurements of uranium enrichment. Appl. Radiat. Isot., 48 (1997) 1525-1528.

Sturm M., Richter S., Aregbe Y., Wellum R., Mialle S., Mayer K., Prohaska T., Evaluation of chronometers in plutonium age determination for nuclear forensics: What if the “Pu/U clocks” do not match?, J Radioanal. Nucl. Chem., 302 (2014) 399-411.

Sweet L. E., Blake T. A., Henager Jr C. H., Hu S., Johnson T. J., Meier D. E., Peper S. M., Schwantes J. M., Investigation of the polymorphs and hydrolysis of uranium trioxide, J. Radioanal. Nucl. Chem., 296 (2013) 105–110.

Tan S., Horlick G., Matrix-effect Observations in Inductively Coupled Plasma Mass Spectrometry, J. Anal. At. Spectrom., 2 (1987) 745-752.

Thompson J. J., Houk R. S., A Study of Internal Standardization in Inductively Coupled Plasma-Mass Spectrometry, 41 (1987) 801-806.

Trešel I., Quétel C. R., Taylor P. D. P, Solution to data integration problems during isotope ratio measurements by magnetic sector inductively coupled plasma mass spectrometer at medium mass resolution: application to the certification of an enriched ^{53}Cr material by isotope dilution, Spectrochimica Acta Part B, 58 (2003) 551-563.

Vanhaecke F., Vanhoe H., Dams R., The use of internal standards in ICP-MS, Talanta, 39 (1992) 737-742.

Varga Z., Wallenius M., Mayer K., Origin assessment of uranium ore concentrates based on their rare-earth elemental impurity pattern, Radiochim. Acta, 98 (2010a) 771-778.

Varga Z., Katona R., Stefánka Z., Wallenius M., Mayer K., Nicholl A., Determination of rare-earth elements in uranium-bearing materials by inductively coupled plasma mass spectrometry, Talanta, 80 (2010b) 1744-1749.

Varga Z., Wallenius M., Mayer K., Hrnecek E., Alternative method for the production date determination of impure uranium ore concentrate samples, J. Radioanal. Nucl. Chem., 290 (2011) 485-492.

Varga Z., Krajko J., Peńkin M., Novák M., Eke Z., Wallenius M., Mayer K., Identification of uranium signatures relevant for nuclear safeguards and forensics, J Radioanal Nucl Chem, 312 (2017) 639-654.

Vaughan M., Horlick G., Oxide, Hydroxide, and Doubly Charged Analyte Species in Inductively Coupled Plasma/Mass Spectrometry, Appl. Spectrosc., 40 (1986) 434-445.

Vaughan M., Horlick G., Correction Procedures for Rare Earth Element Analyses in Inductively Coupled Plasma- Mass Spectrometry, Applied Spectroscopy, 44 (1990) 587-593.

Vesterlund A., Lagerkvist P., Ramebäck H., Study of separation methods and spectral interferences for accurate measurements of lanthanides in uranium-rich samples using ICP-SFMS, 2014, FOI-R--3885--SE.

Wacker J.F., Curry M., Proposed Framework for National Nuclear Forensics Libraries and International Directories, PNNL-SA-70589, 2011.

Wallenius M., Mayer K., Ray I., Nuclear forensic investigations: Two case studies, Forensic Science International, 156 (2006) 55-62.

Wallenius M., Lützenkirchen K., Mayer K., Ray I., de las Heras L.A., Betti M., Cromboom O., Hild M., Lynch B., Nicholl A., Ottmar H., Rasmussen G., Schubert A., Tamborini G., Thiele H., Wagner W., Walker C., Zuleger E., Nuclear forensic investigations with a focus on plutonium, J. Alloys Compd., 444–445 (2007) 57–62.

Waters L.S. (Ed.), MCNPX user's manual, Version 2.3.0. Los Alamos National Laboratory Report LA-UR-02-2607, 2002.

White W., Geochemistry, Wiley-Blackwell, Chichester, UK, 2013.

Williams R. W., Hutcheon I. D., Kristo M. J., Gaffney A. M., Eppich G. R., Goldberg S., Morrison J. J., Essex R., Radiochronometry by Mass Spectrometry: Improving the Precision and Accuracy of Age-Dating for Nuclear Forensics, LLNL-CONF-655059, International Conference on Advances in Nuclear Forensics: Countering the Evolving Threat of Nuclear and Other Radioactive Material out of Regulatory Control, Vienna, Austria, 2014.

United Nations Security Council Resolution (UNSCR) 1540, S/RES/1540, 2004.

Yang Y., Zhang H., Chu Z., Xie L., Wu F., Combined chemical separation of Lu, Hf, Rb, Sr, Sm and Nd from a single rock digest and precise and accurate isotope determinations of Lu-Hf, Rb-Sr and Sm-Nd isotope systems using Multi-Collector ICP-MS and TIMS, Int. J. Mass Spectrom., 290 (2010) 120-126.

Zinn W.H., Szilard L., Emission of Neutrons by Uranium, Phys. Rev., 56 (1939) 619-624.

Zsigrai J., Nguyen C.T., Berlizov A., Gamma-spectrometric determination of ^{232}U in uranium-bearing materials, Nucl. Instrum. Meth. B, 359 (2015) 137-144.